SEPARATION AND CHARACTERIZATION OF MEMBRANES FROM VEGETATIVE, *MYXOCCCOCUS XANTHUS* DK1622 CELLS

by

VESNA SIMUNOVIC

(Under the Direction of Lawrence J. Shimkets)

ABSTRACT

The inability to separate inner and outer membranes in wild-type *Myxoccocus xanthus* DK1622 has been a major obstacle in examining the physiology of this organism. Using spheroplasting in combination with sucrose density centrifugation we now report isolation and characterization of several membrane fractions. Biochemical analysis suggests that these fractions correspond to inner, hybrid and outer membranes. A fifth membrane fraction contains a Ta-1 polyketide synthetase. Two dimensional SDS-PAGE gel analysis indicated the presence of distinct inner and outer membrane proteomes. Using this approach in conjunction with Western blotting, we demonstrate differential localization of several surface-associated proteins required for social motility and signaling.

INDEX WORDS: Membrane separation, Sucrose density centrifugation, Protein localization, Membrane proteome, Polyketide synthetase

SEPARATION AND CHARACTERIZATION OF MEMBRANES FROM VEGETATIVE, *MYXOCCOCUS XANTHUS* DK1622 CELLS

by

VESNA SIMUNOVIC

B.S., Mercer University, 1998

A Thesis Submitted to the Graduate Faculty of The University of Georgia in Partial Fulfillment of the Requirement for the Degree

MASTER OF SCIENCE

ATHENS, GEORGIA

2002

SEPARATION AND CHARACTERIZATION OF MEMBRANES FROM

VEGETATIVE, *MYXOCCOCUS XANTHUS* DK1622 CELLS

by

VESNA SIMUNOVIC

Approved:

Major Professor: Lawrence J. Shimkets

Committee: Timothy Hoover
Eric Stabb

Electronic Version Approved:

Maureen Grasso
Dean of the Graduate School
The University of Georgia
December 2002

ACKNOWLEDGMENTS

I would like to thank Dr. Frank Gherardini for enthusiastic guidance, Dr. Lawrence Shimkets for mentoring and help with thesis writing, Dr. Eric Stabb and Dr. Timothy Hoover for critical reading of my thesis, James Carrol for mass spectrometry analysis, Barry Goldman for computer-assisted analysis of the *M. xanthus* genome, Matt Chenoweth and all members of Dr. Rob Mayer's lab (Adreana, Nalini, Stefan, and Praveen) for unselfish sharing of lab equipment. I would also like to acknowledge my family, and friends, as well as the town of Athens and its bartenders who have kept me laughing over the years.

TABLE OF CONTENTS

Page

LIST OF TABLES

Page

Table

LIST OF FIGURES

Page

Figure

CHAPTER 1

INTRODUCTION

Myxobacteria- Citizens of all Nations. Myxobacteria inhabit most of the Earth's surface (91). The remarkable capacity of these organisms to endure a wide, often extreme range of climates and geochemical conditions lies in their capacity to respond to unfavorable conditions by building environmentally resistant cells called myxospores.

Myxobacteria are primarily soil organisms even though they can also be found in freshwater and saline biotopes (21). Typical myxobacterial species found in soil are *Nannocystis exedens, Corallococcus coralloides, Sorangium cellulosum* and different *Polyangium, Cystobacter,* and *Myxococcus* species. Most frequently myxobacteria inhabit slightly acidic to slightly alkaline soils with a pH between 5 and 8. However, growth in acidic (pH 3.7) or alkaline soils (pH 8.0- 9.2) has also been reported. The same holds true for different types of soils since myxobacteria inhabit organically rich soils, rocky mountain regions, as well as arid, desert soils. Besides soil, this family of organisms is also found on the bark of trees and rotting wood (*Stigmatella aurantiaca, Chondromyces apiculatus, Myxococcus fulvus*), as well as dung pellets of herbivores (predominantly *Myxococcus* and *Cystobacter* species) (21).

Myxobacteria have been isolated on all seven continents. The variance in geographical distribution also encompasses a wide range of climates, ecosystems and altitudes ranging from the tropical rain forests of Latin America and India to central

Algeria. A few psychrophilic species (*Myxococcus fulvus*, *Myxococcus virescens*, and *Corallococcus coralloides*) with temperature growth optima from 0-4°C were isolated from Antarctica, Canada, Alaska, Scandinavia and the Alps. In contrast, numerous myxobacteria have been reported in the Mohavi and Sahara deserts.

Phylogenetic classification. Based on 16S rRNA homology, myxobacteria have been assigned to the delta Proteobacteria. In consent with Bergey's Manual of Systematic Bacteriology, the order *Myxococcales* is arranged into four families: *Myxococcaceae*, *Archangiaceae*, *Cystobacteraceae*, and *Polyangiaceae* (75). The phylogenetic tree reveals two main divisions: one division contains the closely related genera *Myxococcus*, *Stigmatella*, *Archangium*, and *Cystobacter*, while the other division is comprised of four more divergent genera, *Sorangium*, *Polyangium*, *Chondromyces*, and *Nannocystis*. The relatedness of the first four genera is also evident from several other physiological and biochemical characteristics. They are rod-shaped cells with tapered ends that become spherical during myxospore morphogenesis. They move in ripples, produce monocyclic carotenoids, and adsorb the diazo dye Congo red (101). Interest in myxobacteria is divided in two directions. Much basic research is directed towards the molecular mechanisms of fruiting body development. *Myxococcus xanthus* has emerged the model system for this ambitious project. The other more applied direction is secondary metabolite production where *Stigmatella* and *Sorangium* are model systems.

Nutrients and life cycle of *M. xanthus* FB. *M. xanthus* achieves optimal growth in a medium containing a mixture of peptides and amino acids, and a temperature of about 32°C. It is auxotrophic for isoleucine, leucine and valine (22). In its natural habitat, *M. xanthus* generates this carbon pool by collective decomposition of protein or predation on other bacteria. The feeding strategy involves the secretion of numerous hydrolytic

enzymes capable of degrading virtually any biopolymer (12, 13). Like many other gram-negative bacteria, *M. xanthus* grows as thin, long rods (0.7 to 1.2 μm) that divide by binary fission (101). Myxobacteria are unique among prokaryotes for their ability to respond to nutritional stress by initiating a developmental program that engages whole cell populations rather than single cells. Thus, development is not the inevitable result of growth but an evolutionary defense (101).

During development tens of thousands of cells migrate toward the aggregation foci where they undergo morphogenesis. The process of aggregation can be separated in two morphologically distinct phases that are cell-density dependent. The first phase is characterized by low-density arrangement of cells and results in the formation of traveling waves. As the cell density increases, ripples converge into sheets of cells that pile on top of each other to form hemispherical mounds called fruiting bodies. Within fruiting bodies individual cells convert to spherical cells called myxospores, which are dormant cells capable of resisting extreme temperatures, nutrient limitation, and desiccation (109). Once favorable growth conditions have been restored, myxospores germinate and give rise to a new generation of rod-shaped vegetative cells.

Development of *M. xanthus* is astonishing in view of the fact that morphogenesis appears to be an energetically demanding process that calls for programmed cell death of about 80% of members of the initial population. Only about 10% of the cells become environmentally resistant spores, while another 10% of the cells remain rod-shaped cells and reside between fruiting bodies (82).

Motility. All myxobacteria move by gliding, a smooth translocation of cells over the solid surface or water-air interface that results in the formation of colonies with characteristic peninsular-like spreading edges. Gliding cells generally move along their long axes utilizing mechanisms that do not require flagella (71). In *M. xanthus*, the

interplay of two distinct genetic motility systems, the social (S) system and the adventurous (A) system, facilitate gliding.

The social (S) motility system involves group movement, which is reduced in S mutants. Additionally, most S mutants are defective in fruiting body formation (40). Social motility in *M. xanthus* resembles twitching motility of *Neisseria gonorrhoeae* and *Pseudomonas aeruginosa.* This type of movement is mediated by extension, attachment, and retraction of type IV pili (tfp) (76, 106, 110). Conservation in tfp biogenesis is evident from the fact that 14 out of 17 *M. xanthus* putative products of a tfp gene cluster have homologues in the *P. aeruginosa* genome (71). These include the basic structural pilin subunit protein encoded by *pilA*, *pilD*, which encodes a bifunctional prepilin peptidase/ C- terminal methylase, *pilB*, *C*, *M*, *N*, *O*, and *P* genes which encode proteins engaged in the polymerization process, and a *pilQ* homologue (formerly known as *sglA*) which encodes a putative channel in the outer membrane.

Pilin production is controlled via a PilS/ PilR two-component signal-transduction system, while PilT may act as the actual motor by using ATP hydrolysis to retract the pili and thus generate net movement over the surface. However, tfp biogenesis in *M. xanthus* requires two unique elements: an ATP-binding cassette transporter encoded by the *pilG*, *pilH*, and *pilI* genes (128), and the Tgl lipoprotein (93). Many other gene products, such as LPS O-antigen (10), and products of the *dsp* locus, also known as the *dif* locus (61) are required for social gliding, whereas products of the *frz* system facilitate, but are not essential for, social motility. The products of *frz* and *dif (dsp)* bear substantial homologies to the chemotaxis genes of *E. coli* (71).

The *frz* chemotaxis gene cluster regulates the directionality of gliding movement (120). Wild-type cells reverse direction every 5-7 minutes. During fruiting body formation the reversal period is gradually reduced to allow proper aggregation of cells

into fruiting bodies. The *frz* mutants show a severe defect in aggregation represented by tangled (frizzy) aggregates (120).

Whereas the *frz* gene products regulate reversal frequency, the *dsp* (*dif)* chemotaxis system appears to encode components of a signal transduction pathway that regulates the production of fibrils, yet another appendage-like organelle found on the *M. xanthus* surface (120). Fibrils purified from wild-type cells by partial solubilization of the membrane in SDS were shown to consist of a polysaccharide backbone decorated with proteins (4). In their native state, fibrils are extruded from many points along the cell and extend to 50 μm in length and 15-30 nm in diameter (71). Fibril production is stimulated by either of two means: starvation (2) or cell contact (5). The regulation of fibril synthesis is not very clear. However, fibrils appear to be negatively regulated by FibR, a protein that contains homology with a repressor of alginate biosynthesis in *P. aeruginosa* (122). The *sglK* gene product encodes a homologue of the chaperone HSP70 that also plays an important role in social motility (122).

The adventurous or A motility system allows movement of single cells independently of the swarm, and is best manifested on relatively dry and firm surfaces such as 1.5% agar (97). Cells carrying mutations in the A motility system lack movement of isolated cells, but many mutants still form fruiting bodies using the S system (39, 40, 68). A defect unique to A^- mutants lies in their inability to sense and respond to elastic forces on hard surfaces, a phenomenon known as elasticotaxis (25). The normal elasticotactic response entails repositioning of cells along the lines of stress to minimize their impact. At least 5 *cgl* (conditional gliding) loci have been discovered whose motility can be rescued by co-development with wild-type cells. In addition, 32 *agl* (adventurous gliding) loci (39, 40, 68) have been described whose defects cannot be rescued by contact with agl^+ cells. To date, only two genes (*cglB* and *aglU*) have been

characterized and both encode putative outer membrane lipoproteins (92, 124). Several possible mechanisms of A motility have been proposed.

The mechanism proposed by Lunsdorf and Reichenbach argues that periodically positioned ring-like, helical structures generate the gliding motion by formation of "contractile waves" (66). The ultrastructure was absent in A mutants (66) or mutants completely blocked in motility (67). Another model proposes that expulsion of slime, a hypothetical electrolyte, through polar nozzles, powers individual cell movement (125). Elucidation of the mechanism of A motility is yet to come.

Cell-cell signaling in *M. xanthus*. Reorganization of a flat cell layer to form complex structures requires intercellular communication or the ability of individual cells to communicate with siblings via exchange of signals (103). In this respect, cell signaling acts as the informational current that synchronizes and modulates cell behavior. In *M. xanthus*, development depends on the exchange of at least five signaling molecules. Production of each signal is abolished in one of the six conditional mutant groups. While all conditional mutant groups fail to sporulate, their developmental defect is alleviated when they are mixed with other mutant groups or wild-type cells. Accordingly, development is thought to be based on the extracellular exchange of specific signals. In the past two decades, attempts have been made to clone and identify the genes responsible for mutant phenotypes with the hope that they would carry mutations in genes encoding the actual signals. These efforts, however, did not identify the signals. Table 1.1, which gives a comprehensive list of genetic loci responsible for A, B, C, D, E, and S conditional mutant groups, shows that most genes encode regulatory proteins, and few enzymes. Below follows a synopsis of each of the complementation groups, with special emphasis on the C mutant group.

The A-mutant group. The A complementation group contains members with mutations in one of five unlinked loci, four of which encode regulatory proteins. AsgA is a hybrid protein that contains both a histidine kinase domain and a response regulator domain of a two-component system (89). *asgB* encodes a putative transcription factor of unknown function (90) while *asgC* encodes the major sigma factor, σ-70, a homologue of *E. coli rpoD* (20). A potentially interesting role of AsgC in starvation sensing was proposed after isolation of the *asgC767* allele bearing a glutamate-to-lysine mutation in the conserved region 3.1 (20). A mutation that localizes to an adjacent codon in *E. coli* RpoD suppresses a *ΔrelAΔspoT* mutation and is believed to be responsible for (p)ppGpp-mediated gene regulation. The *asgD* locus codes for another putative two-component regulatory system with an amino-terminal receiver domain and a histidine kinase at the carboxy-terminus (16). An unusual characteristic of *asgD* is that it fails to recognize partial starvation when plated on CF starvation media. However, when casitone, citrate, and pyruvate are eliminated from CF agar (MCC media) to produce more extreme starvation, the *asgD* mutant produces 33% of the wild-type level of spores. In addition, alanine, leucine, and serine rescue development on CF media. Together, these results underline the role of *asgD* in sensing nutritional status during early development (16).

A novel locus belonging to the A-mutant group was recently discovered (26) and shown to consist of two genes: *asgE* and *orf2*. While *asgE* is expressed both during vegetative growth and development, *orf2* is transcribed exclusively during development. *asgE* initiates transcription around 6 hours into development and reaches peak activity at 24 hours. It is positively regulated by *relA*, *asgA*, *asgB*, *asgC*, and *csgA* and is required for production of proteases during early development. Several attempts to model the interplay of *asg* regulatory proteins in sensing starvation and transcriptional activation of early developmental genes have been made but the actual mechanism remains unknown (90).

A-signal. The *asg* mutants can be rescued by addition of A-signal, which consists of about 15 amino acids present at an average concentration of 25 μM, or extracellular proteases that are responsible for protein and peptide degradation (59). Amino acids with the most A-signal activity are tyrosine, proline, phenylalanine, tryptophan, leucine, isolecine, and alanine. Surprisingly, an exact stoichiometric ratio of the amino acid species in the A-signal cocktail is not required since one amino acid can be replaced by a higher concentration of another.

Perhaps the most striking feature of A-signal is that its production rises in a linear fashion with the cell density. This conclusion was confirmed indirectly by measurement of A-signal dependent reporter gene Ω4521 fused to *lacZ*. When cells were present at low cell density (2×10^8 cells/ml), reporter expression reached 25% of its maximum activity. A five-fold increase in cell density yielded maximum gene expression. A-signal acts directly as a detector of cell density since addition of high amounts of A-signal to cells present at low density stimulates full expression of ΩDK4521 (59). Assessment of the number of starving cells through A-signal is believed to provide information on whether the cell pool is large enough to construct a fruiting body (103).

The A-signal response pathway. Using Tn*5 lac* transposition, Kroos and co-workers identified 18 genes with at least three-fold increase in expression during development, but with greatly reduced expression in an *asg* mutant (57). These genes started being transcribed about 1.5 hours into development and were termed A-signal dependent. Recent insights into the mechanism of perception of A-signal amino acids came from studies of Tn*5 lac* Ω4521, which appears to be expressed under control of σ-54 (51) and requires environmental signals carrying information with regard to nutrient levels and

cell density status. Suppressor mutations that restore Ω4521 expression disclose complex regulatory circuitry (90). They mapped to two loci: *sasA* and *sasB*. *sasA* locus consists of three genes that encode a putative ATP-binding cassette transporter (*rfb ABC*, previously designated as *wzm*, *wzt*, and *wbgA*) (34). Besides acting as suppressors of Ω4521 gene expression, mutations in *sasA* also block LPS O-antigen synthesis, abolish social gliding motility, and give rise to aberrant fruiting bodies bearing low levels of spores (10, 34). Four genes were identified in the *sasB* locus: *sasS*, *sasR*, *sasN*, and *sasP* (35). The *sasS* gene product bears similarity to the methyl-accepting chemotaxis protein receptor (MCP) family of *E. coli* in its N terminus. The carboxy terminus of SasS encodes a typical histidine kinase domain (86). SasS appears to play an important role in sensory transduction since a *sasS* null mutant produces normal levels of A-signal but is unable to respond to the signal. Additionally, SasS contains a gain of function amino acid substitution, E139K, in the periplasmic region that serves as a known ligand receptor in *E. coli* histidine kinase proteins (90). This raises the possibility of SasS acting as a direct sensor of A-signal amino acids or, alternatively, through interaction with other membrane bound amino acid sensor proteins. The second suppressor mutation localizes to *sasR*, which encodes an NTRC-like response regulator. Epistasis experiments demonstrate that SasR acts downstream of SasS (129). The third suppressor mutation localizes to *sasN*, which encodes a negative regulator of Ω4521 during vegetative growth. The last suppressor allele *sasP* encodes a protein of unknown function (35).

B-group. The B-mutants carry a mutation in a single gene, *bsgA*, which arrests development very early (30). The BsgA amino acid sequence resembles that of the *E.coli* Lon family of ATP-dependent proteases (31, 113). Bsg has been found to localize mainly in the cytoplasm, with minor amounts (5-10%) associated with the membrane (30). Western blot analysis indicates rather constant levels of Bsg during the first 12

hours of development, thus making it difficult to anticipate a role in development or B-signal production. Despite many unknowns surrounding BsgA, including identification of its substrate, BsgA has been shown to act as a positive regulator of *csgA* expression as *bsgA* cells transcribe 50% less *csgA* (18). A single *bsgA* suppressor mutation has been isolated so far. It is localized to the *spdR* gene, which encodes a two-component transcriptional regulator of an NTRC family (37).

D-group. The *dsg* mutant terminates the developmental program during early aggregation. This complementation group contains mutations in a single gene, named *dsgA*, which encodes translation inititation factor 3 (IF3), a protein that assists in the selection of the initiation codon. The function of Dsg as an initiation factor has been confirmed *in vivo* (48). Like other initiation factors, Dsg is essential for cell viability (15) and is present at constant levels throughout the life cycle (48). The two alleles, *dsgA429* and *dsgA439*, grow normally (15). Kalman and Kaiser proposed that viable *dsg* mutants fail to translate mRNA involved in synthesis of the D-signal as well as other genes. This model accounts for other *dsg* pleiotropic defects such as lack of yellow pigmented, swarming colonies as well as increased DNA uptake capacity. A possible explanation for an increased transformation frequency was proposed to be due to *dsg* increased membrane permeability (48).

Rosenberg's lab showed that the AMI fraction, which mainly consists of phosphatidylethanolamine (PE) breakdown products, such as fatty acids, corrects the *dsg* developmental defect (66). Unlike the model of Kalman and Kaiser, this study suggests that the *dsg* mutant makes D-signal but fails to export it due to the decreased permeability of mutant membranes. Accordingly, insertion of fatty acids in the lipid bilayer restores membrane permeability. Thus, the Rosenberg model also predicts inhibition of A, B, and C signal export which does not occur since a *dsg* mutant complements *asg*, *bsg*, and *csg*

mutants. It is unlikely that D-signal is a mixture of fatty acids since cells do not produce AMI during early development, when *dsg* mutants arrest development. Production of AMI fatty acids starts around 24 hours into development and reaches the peak 72 hours after initiation of development (95).

E-group. E-mutants carry a Tn*5* insertion in the *esg* locus, which codes for an enzyme involved in primer production for branched-chain fatty acid biosynthesis. Specifically, *esg* encodes E1 dehydrogenase that converts leucine, isoleucine and valine-derived branched chain keto acids to their acetyl-CoA derivatives (112). The *esg* mutant is blocked between 3-5 hours in development, thus acting after A-signal and before C-signal. Mutant development is rescued by addition of 1 mM isovalerate (IVA) which restores production of the iso odd fatty acid family including the major fatty acid 15:0. Curiously, *esg* mutants, like *dsg* mutants, contain reduced levels of yellow pigment. Pigment production is also rescued by addition of 1 mM IVA, 2-methylbutyric acid (MBA), and isobutyric acid (IBA). An *esg*::Tn*5* gene disruption reduces growth rate, but is not lethal. In light of these findings, Toal and Downard have proposed that the *esg* products, short-chain fatty acids, are used in the production of long branched-chain fatty acids such as those found in phosphatidylethanolamine (PE) (112).

C-group. All mutants incapable of producing C-signal have a lesion in a gene known as *csgA* (99, 100). From *csgA*, two other open reading frames extend divergently, both of which encode gene products that participate in anabolic reactions. Downstream from *csgA* is *fprA*, which encodes a flavin mononucleotide (FMN)-dependent enzyme. Based on sequence homology this protein may catalyze a step in the production of the coenzyme pyridoxal 5'-phosphate (60). Upstream of *csgA* is *hemG* which may encode protoporphyrinogen oxidase (19). Both proteins are essential for normal cell growth (98)

and both proteins require coenzymes for their catalytic activity (FMN and FAD, respectively). Despite the fact that the *fprA* and *csgA* transcriptional units overlap (36), and the fact that *hemG* and *csgA* use overlapping divergent promoters, the effect of *hemG* and *fprA* on *csgA* expression is probably insignificant due to the low levels of *hemG* and *fprA* expression throughout the life cycle.

Nature of C-signal and its mechanism of action.

C-signal: small molecule or a peptide? CsgA is a 24.8-kDa protein with homology to the short chain alcohol dehydrogenase family (63). Production of a shorter, proteolytically cleaved form (17-kDa), is also evident under submerged culture conditions starting about 3 hours into development (58). Fundamental questions regarding the

C-signal still wait to be discerned. First of all, what is the C-signal? Two opinions have emerged: one argues that the C-signal is a small biochemical, and the other proposes that the C-signal is the hydrolyzed 17-kDa form of CsgA.

The model favored by our lab is based on the idea that CsgA is an enzyme whose enzymatic product acts as the C-signal. Several lines of evidence contribute to this theory. Primarily, CsgA bears homology to the family of short chain alcohol dehydrogenase family (SCAD) (3). This ubiquitous family of enzymes bears two signature sequences, one located at the amino terminus involved in $NAD(P)^+$ binding and the other located in the active site. Consistent with these sequence results, Lee and coworkers performed site-directed mutagenesis of conserved residues and confirmed the indispensable nature of both the $NAD(P)^+$ and catalytic domains (63). Specifically, mutations in the key $NAD(P)^+$ binding residues, T6A and R10A, failed to develop and yielded fewer than 1% of the normal number of spores. In addition, MalE-CsgA T6A has reduced affinity for NAD^+ in an *in vitro* binding essay. Addition of 10 μM $NAD(P)^+$ to

csgA cells premixed with biochemically active MalE-CsgA increased sporulation another 20% thus bringing this value close to the wild-type sporulation level. In contrast, addition of 10 μM NADH delayed sporulation for 24 hours while reducing sporulation frequency 10%. Parallel with these results, mutations in the substrate binding pocket, S135T and K155R, also failed to develop while a MalE-CsgA S135T protein, unlike MalE-CsgA, was not able to complement development of *csgA* cells.

Another independent line of evidence underlining potential enzymatic action of CsgA was gathered from *csgA* suppressor mutations localized to the *socABC* operon (64). Transposon insertion *soc559* disrupts putative DNA-binding protein SocC causing 100-fold overexpression of *socA* during growth and development. SocA encodes a short chain alcohol dehydrogenase with only 28% identity to CsgA. These data, combined with the observation that co-development of *socC csgA* cells complement *csgA* development support the possibility that SocA compensates for the lack of CsgA by producing the C-signal (64).

A third line of evidence in favor of CsgA acting as an enzyme stands out from the study of CsgA in relation to the stringent response. Crawford demonstrated that silencing of SocE, a protein that negatively regulates CsgA, induces sporulation under conditions of agitated growth in a nutrient rich media. Sporulation was abolished when the wild type *csgA* allele was replaced with *csgA* alleles carrying the T6A and S135T point mutations. Thus, CsgA can drive development without a requirement for cell-to-cell contact, previously believed to be a prerequisite for C-signaling (18).

The second model, developed by Kaiser's group suggests that the C-signal is the 17-kDa form of CsgA. This protein has been purified from developing wild-type membranes based on its ability to enable *csgA* cells to successfully progress through all morphologic stages of development, and to induce C-signal-dependent gene expression (52, 53). A fraction enriched in C-factor has also been shown to give input to the *frz*

transduction system (107). However, the same molecular effects can occur by addition of a MalE-CsgA hybrid protein that contains full length CsgA (24.8-kDa). MalE-CsgA was also found to directly modify the motility behavior of *csgA* cells by increasing the transient gliding speed and timing of the gliding interval while decreasing the mean stop interval (41).

C-signal transmission requires motility and direct cell-cell contacts. Perhaps the most obvious paradigm demonstrating this point comes from an experiment by Kim and Kaiser (55). *mgl* cells, which lack motility, and motile, *csgA* cells abort development at a similar, if not identical stage. Kim and Kaiser designed an experiment using a *mgl* strain containing Tn5 *lac* fusion with a C-signal dependent gene. The logic behind the experiment was that while *mgl* cells are defective in motility they produce normal levels of CsgA but fail in its transmission. Using grooves within the agar, they aligned the cells mechanically so as to achieve packing with the maximum end-to-end and side-by-side contact. Cells residing outside the grooves adopted a random orientation. Three days post development, cells within the ridges exhibited visually distinctive blue stripes due to β-galactosidase production, while the randomly oriented cells remained yellow. Ovoid spores that formed following five days of starvation thus demonstrated that bypass of the motility defect through direct contact established conditions for C-signaling. While addition of the purified C-signal allows nonmotile *mgl* cells to sporulate and express C-signal dependent set of genes, a classical complementation test involving co-development of *mgl* and *csgA* mutants does not engage cells in fruiting body construction, underlining the essentiality of motility for *M. xanthus* development (54).

CsgA localization. Depiction of the proper model of C-signaling is directly dependent on the correct cellular localization of CsgA during growth and development. An early

study by Shimkets attempted to address this using immunolocalization (102). In this study, cells starved for 18 hours were reacted with CsgA antibody and prepared for scanning electron microscopy. This approach revealed 1100-2100 CsgA molecules per cell associated with the extracellular matrix. Another study by O' Connor found CsgA associated with membrane vesicles (80). Membrane vesicles (MV) are spherical membrane structures 50-250 nm in size, which contain encapsulated fragments of outer membrane and periplasm (7). These structures, common to many Proteobacteria, are produced under both liquid and solid growth conditions. A fascinating feature of MVs is that they can reconstitute themselves back into the membranes of living cells via adhesion and integration (46). Electron microscopic observations of vegetative *M. xanthus* cells revealed an abundance of MVs (6). However, it is still not clear how similar *M. xanthus* vesicles are to other well-characterized vesicles, such as those of *P. aeruginosa*. Nonetheless, evidence of CsgA present in these little hydrophobic islands opens up the possibility of a novel mechanism of signal exchange.

CsgA as the developmental timer. Several previous studies have demonstrated that CsgA acts as a developmental timer. Li and co-workers measured *csgA* expression in a *csgA-lacZ* fusion strain and compared expression in strains with truncated upstream regulatory regions (65). Experiments also examined expression under conditions of extreme starvation and less rigid starvation with low levels of carbon and nitrogen compounds (CF media). Results of this study demonstrated that maximum *csgA* expression requires 400 and 930 bp upstream from the start of transcription, in respect to the extreme and less rigid starvation conditions, indicating specific roles of each DNA segment in sensing the nutritional status of the cell. Under both starvation conditions increases in the length of the deletion reduces *csgA* expression in a proportional fashion. Thus, by manipulating levels of *csgA* expression Li and co-workers suggested that each

morphological stage of development can be induced by a specific level of *csgA* expression. Rippling is induced with less than 20% of the maximum CsgA expression; aggregation requires 30% of maximum expression, while sporulation requires 80% activity.

Addition of purified 17-kDa CsgA, also known as C-factor, to *csgA* mutant cells submerged in a starvation buffer had a similar effect. Addition of 0.8 units of purified protein restored aggregation and transcription of early C-signal-dependent genes while the addition of 1 unit enables cells to complete development and induces transcription of the late developmental genes (52). Thus, 1 unit is the amount of protein that restores development to 2 x 10^7 cells/ml. In contrast, CsgA present in concentrations above 1 unit inhibited development. Similar results were obtained by the addition of purified full length CsgA (24.8-kDa) containing MalE at the amino terminus. Hybrid MalE-CsgA succeeded in restoring *csgA* mutant sporulation up to 80% of the wild type at a 100 nM concentration (63).

M. xanthus cells engineered to produce 10-fold higher levels of CsgA begin aggregating about 6 hours earlier than wild-type cells. Moreover, the presence of many small mounds without ripples in between, and the presence of small fruiting bodies also characterize the developmental phenotype of the overproducing strain. Phenotypic characterization along with immunoblot quantification data corroborate that overdosing of CsgA during development abolishes rippling, accelerates fruiting body formation and sporulation, and results in the production of undersized fruiting bodies. However, excess CsgA does not alter the final spore yield (58). Use of Western blotting gave the first opportunity to create expression profiles of both protein forms *in vivo* thus giving insight into the dynamics of CsgA production and cleavage. In addition, CsgA levels in wild- type cells increase gradually to reach peak activity at 12 hours of development. The cleaved form of the CsgA (17-kDa), becomes detectable in Western blots at 3 hours,

reaches its maximal production at 12 hours and is undetectable again by 18 hours. The short form of the protein is present at 10-fold lower concentrations compared to the full-length form, and appears to be specific to the aggregation phase of development (105). The significance and possible functions of this peptide will be discussed later in this chapter.

Regulation of *csgA* expression. Known regulators of *csgA* expression are *csgA* itself, *bsgA*, genes of the *act* operon, *socE* and *relA* genes. Autoregulation of *csgA* expression was suggested in earlier work by Kim and Kaiser (52). Using a *csgA* mutant strain that contains a *csgA* transcriptional fusion with *lacZ* (100), β-galactosidase specific activity was monitored in *csgA* cells, as well as *csgA* cells mixed with either wild-type cells or CsgA itself. Whereas *csgA-lacZ* cells starved independently retained constant level of β-galactosidase expression, *csgA-lacZ* cells co-developed with wild-type cells or with CsgA had about four-fold increase in β-galactosidase expression during development, suggesting involvement of *csgA* in a positive feedback loop. (52). Another positive regulator of *csgA* is *bsgA*. *bsgA* mutation results with 50% reduction in *csgA* expression (63). The manner in which this protease elicits such a response has not been investigated.

Finally, genes clustered in the *act* operon are part of the *csgA* regulatory circuitry (33). *actA* encodes a putative histidine kinase while *actB* encodes a putative σ-54-dependent activator protein of the NTRC family. *actC* contains an internal fragment that resembles members of N-acetyltransferase protein family and *actD* codes a protein of unknown function. Even though all four genes are cotranscribed, phenotypic assessment implied that *actA* and *actB* deletion mutants continued rippling even during late aggregation and were completely defective in sporulation, while *ΔactC* and *ΩactD* aggregated normally but produced only about 18-19% of the wild type level of spores. These developmental defects were directly correlated with levels and timing of CsgA protein production as detected by Western blotting. While *actA* and *actB* synthesized

only 25% of the protein present at any time point in normal cells, *ΔactC* and *ΩactD* made ~95% of wild-type protein level in an improper temporal order. Thus, the *act* operon regulates levels of *csgA* expression (*actA* and *actB*) as well as timing of its production (*actC* and *actD*). *actA* and *actB* are the first sensory proteins likely to play a direct role in the regulation of *csgA*. Even though *csgA* upstream region does not have the σ-54-dependent sequence, *actB* might regulate *csgA* expression directly by binding enhancer sequences upstream from *csgA* (33). This hypothesis is based on the recent discovery of σ-54 independent sequence requirement of a response regulator found in *Rhodobacter capsulatus* (121). Regulation of *csgA* by *socE* and *relA* gene products will be discussed in the following section in the context of the stringent response.

Stringent response. Following nutrient deprivation, many gram-type negative bacteria induce a specialized metabolic response known as the stringent response. Amino acid limitation halts synthesis of stable RNA in response to uncharged tRNA. GTP is diverted to the ribosome-associated enzyme RelA which initiates synthesis of (p)ppGpp using ATP and GDP (GTP) molecules as precursors. Elevated levels of (p)ppGpp act as a global intracellular signal that alters transcription and enzyme activity. The effects of (p)ppGpp alarmone action results in inhibition of processes related to growth such as DNA and stable RNA synthesis (14), and cell division (116). It also increases and attempts to alleviate nutritional stress by upregulating amino acid biosynthesis and transport (14).

Analogous to *E. coli*, initiation of the stringent response is a necessary prerequisite for sensing amino acid starvation in *M. xanthus*. The *relA* genes of the two organisms share 49% identity and 75% similarity. More important, ectopically expressed *relA* of *E. coli* rescues a *M. xanthus* relaxed (*relA*) mutant as measured by (p)ppGpp production using thin layer chromatography (38). However, besides executing growth

arrest in response to starvation, the *M. xanthus* stringent response has a central role in deciding developmental fate. During early starvation, the stringent response activates A-signal dependent proteases that produce A-signal (38). However, the very nature of A-signal (mixture of amino acids) creates a potentially paradoxical and doubled-edged situation. Whereas A-signal amino acids act as quorum sensors, gathering the information regarding cell population density, they simultaneously act as the food source. This assumption is supported by the fact that as the cells reach 5 x10^9 cells/ml, the concentration of A-signal amino acids approaches the value found in growth medium. Thus, it is likely that additional gene regulation is required to fortify the starvation signal and allow metabolic switching from the vegetative to the developmental cycle. This regulation is achieved in perplexing interactions of *relA*, *socE*, and *csgA* gene products.

Stringent response activates *csgA* while repressing *socE*. Measurements of *csgA* and *socE* mRNA levels deduced from slot blots or as transcription from their corresponding *lacZ* fusions, show inverse patterns of gene expression. While *socE* expression is high during vegetative growth and drops during early development, *csgA* expression is low during vegetative growth but increases during development to reach a peak at 72 hours of development. These data, in conjunction with constantly high levels of *socE*, and constantly low levels of *csgA* in *relA* backgrounds, argue that activation of *csgA* is dependent on the stringent response (18).

SocE inhibits CsgA and RelA. Using ectopic expression of *socE* fused to the light inducible promoter *phv* introduced in the wild-type background, a system was created which allowed *socE* transcription in the presence of light. Silencing of *socE* forced cells to sporulate after 12-15 hours in amino acid rich liquid media. Timing of induction of development corresponded well with decline in stable RNA and DNA synthesis, as well

as with the increase in (p)ppGpp pool (17), all symptoms of stringent response. Induction of *socE* by exposure to light alleviates all the aforementioned phenomena. Sporulation that resulted from *socE* depletion argues that *socE* is a negative regulator of *csgA*. This notion was further strengthened by the observation that levels of *csgA* mRNA are about 30% higher in a conditional *socE* mutant than in the wild-type strain (18). Indirect evidence suggests that CsgA and the stringent response create a positive feedback loop. Comparison of ppGpp levels in wild type, *csgA socE*, a *socE* conditional mutant, and *csgA* following 12 hours of growth in the dark revealed that a strain depleted of *socE*, unlike other three strains, displayed ten-fold higher ppGpp levels. Since *socE* repression upregulates *csgA*, and since the only difference in the four strains is the presence of the functional *csgA*, this leads to the conclusion that CsgA induces a stringent response.

C-signal transduction. Although rippling, aggregation, fruiting body formation and sporulation represent consecutive stages in *M. xanthus* development, the signal transduction pathway that propels these events in the proper temporal order is not linear. This was suspected in the early studies by Morisson and Zusman (79), and Zusman (133) who were the first to isolate mutants that could aggregate normally but failed to sporulate and vise versa, those that were defective in aggregation but successful in sporulation. It is well-established that all four morphogenetic stages are induced and guided by progressively increasing amounts of C-signal, the product of CsgA protein. However, how does the C-signal orchestrate these events?

Reconstruction of the C-signal transduction pathways was initiated after the isolation of two classes of mutants that ceased development at a point similar to *csgA*. These mutations were mapped to the *fruA* and *frz* loci. FruA, a putative DNA-binding response regulator was found to be required for cell movement, C-signal dependent gene expression, as well as sporulation (23). *frz* genes, on the other hand, appeared to control

only movement responses (104). As each mutation has a distinct phenotype, epistasis experiments were used to establish sequential action of *csgA*, *fruA*, and *frz* genes, giving *fruA* the central position (Figure 2.1). From *fruA* two branches extend: one leading to *frz* to control motility reversal responses, and the other leading to sporulation-specific operons such as *devRS* to coordinate sporulation (42).

C-signal acts through the Frz transduction system to modulate cell motility parameters. The *frz* locus regulates the reversal frequency of gliding (73). The *frz* genes encode many structural and functional homologues of the chemotaxis proteins in *E. coli*. Despite the functional differences between swimming behavior in enteric bacteria and gliding of *M. xanthus*, the biochemical basis for the transmission of environmental stimuli relies on the same principle of phosphate transfer between proteins. Consequently, phosphorelay flux is reflected in changes in FrzCD methylation. Changes in FrzCD methylation can be monitored by slight differences in the electrophoretic mobility of methylated versus nonmethylated forms. Analysis of comparative immunoblots of wild-type and *csgA* developing cells probed with FrzCD antibody clearly indicate that CsgA regulates FrzCD methylation (107). In wild-type cells FrzCD becomes fully methylated by 12 hours. Methylation declines to nearly undetectable levels by 18 hours of development and beyond. In *csgA* cells FrzCD methylation is delayed for 12 hours and the methylated protein form persists until 36-hours into development. Addition of 1 unit of purified 17-kDa CsgA or 4 units of MalE-CsgA fusion protein to the previously starved *csgA* cells restored development and induced FrzCD methylation suggesting that C-signal has direct input in the *frz* system (107).

The effects of C-signal on *frz* signal transduction were examined with behavioral assays (41). Individual *csgA* cells stimulated with 1 unit of MalE-CsgA displayed increased transient gliding speeds, reduced stop intervals, and increased gliding intervals. In contrast, *frz* and *frz csgA* mutants had a dramatically reduced response. A high cell

density population of C-signal competent cells is required for reduction of cellular reversal frequency during development (43).

Fluorescent microscopy of a 1:400 mixture of green fluorescent protein (Gfp)-expressing *csgA* and non-fluorescent wild-type cells demonstrated behavioral correction of *csgA* cells (41). Monitoring of a 1:400 mixture of Gfp-expressing wild-type cells and *csgA* cells displayed behavior similar to *csgA* cells. These findings reveal that the C-signal modifies gliding motility to increase the transient gliding speed, reduce the stop intervals, and increase the gliding intervals. Reduction in cellular reversal frequency becomes evident at high cell densities. Reduction of the cellular reversal frequency in combination with the increase in the transient gliding speed changes the pattern of cell movement from oscillatory to unidirectional, eventually allowing formation of a nascent fruiting body.

Devilish *dev* operon expression. The other branch of the C-signal transduction pathway goes through FruA and the *dev* gene cluster to induce transcription of genes required for sporulation. The *dev* operon contains three genes (44), (*devT, devR,* and *devS*) that have been partially characterized. Mutations in all three genes form loose, translucent aggregates yielding only 0.2-1% of the wild-type level of spores.

DevR appears to negatively regulate *dev* operon expression as judged by *devR*::*lacZ* expression in a *dev* and *dev/dev*$^{+}$ background. This argument is further strengthened by quantitation of mRNA levels at 0, 12, and 24 hours of development. Significantly higher levels of mRNA were detected in *dev* than in the *dev/dev*$^{+}$ strain. These experiments also suggested that the *dev* operon retains a low expression profile. *dev* expression is initiated at the onset of aggregation (6 hours) and reaches maximum activity during the fruiting body formation (26 hours) (111).

Using a fluorescence-activated cell sorter (FACS), and a *devR*::Tn*5 lac* transcriptional fusion, Ω4473, Marie-Russo and co-workers measured *devR* expression with the substrate fluorescein di-β-galactopyranoside (96). After 2 hours of starvation Ω4473 cells were sorted in two distinct populations: one contained about 75 % of the cells and displayed high fluorescence while the minor subpopulation emitted little fluorescence. The dual fluorescence distribution persisted at least 10 hours. This experiment suggests partitioning of *devRS* expression at 2 hours into 2 cell types. In addition to the dual mechanisms of *devRS* regulation, early differential expression is suspected to provide a switch-like quality to the *dev* operon. This might provide timely and efficient expression of genes required for closure of the aggregation phase of development and initiation of sporulation.

CsgA regulates *dev* expression. Clearer insights into the *dev* operon expression were provided by Julien and co-workers (45). In this study, the *dev* operon was fused to the (Gfp), and Dev localization was examined by microscopy at 24 hours of development. At this time, Dev-Gfp was localized to the fruiting bodies and no peripheral rods were visibly fluorescent. This observation coincided with 2-3 times higher levels of CsgA present in fruiting bodies than in the peripheral cells by Western blot analysis. Measurement of β-galactosidase activities from four other C-signal dependent genes indirectly revealed 3-4 times higher CsgA expression associated with fruiting bodies. A-signal dependent genes did not follow this expression pattern. Thus, it appears that many differentially expressed genes, including *devRS*, depend on C-signaling.

In general, the studies cited above seem to be in agreement. The 75-80% of cells that expressed *devR* highly as detected FACS could be the cells that eventually form a fruiting body. Accordingly, the remaining cells that expressed *devR* poorly could become

peripheral rods. This calculation is in a good agreement with data suggesting that 10-20% of cells become peripheral rods (81).

DevT acts upstream from *fruA*. Immediately upstream of *devRS* is *devT* (11). DevT, calculated to be a protein of about 56-kDa, has been demonstrated to stimulate transcription of *fruA* as evident by production of β- galactosidase from the *fruA::lacZ* fusion. Additionally, *devT* produces significantly lower amounts of FruA as compared to the wild-type strain. Together, these data indicate that *devT* acts upstream from *fruA.*

Still, more questions remain to be answered regarding studies involving *dev* genes. First of all, does the *dev* operon belong solely to the second branch of the C-signal transduction pathway? A previous study by Thony-Meyer demonstrated that co-development of *dev* with a *dsgA429* strain, characterized by a 2-day delay in aggregation, abolished aggregation altogether, thus highlighting the involvement of *dev* in aggregation (111). This evidence, in conjunction with the latest work showing upstream action on *fruA* by DevT (11) sheds doubt on the present model, which suggests that *dev* has no control over the aggregation-specific pathway. Furthermore, DevT is also necessary for proper methylation of FrzCD during development (11).

Another inconsistency comes from Thony-Mayer's data showing reduction in *dev* expression with an increase in cell density, as measured 24 hours after inititation of development (111). These data are in contradiction with both β-galactosidase expression of *dev::lac* fusions as well as *dev-gfp* localization data, both of which indicate highest *dev* expression at high cell densities. Even the fact that 20% of the cell population do not express *dev* cannot account for these discrepancies.

Thesis project. Examination of social and adventurous motility, as well as developmental cell signaling has been hampered by the lack of a general approach to

observe protein localization, and transport across membranes, or identify surface receptors. The goal of my project is to find an optimal approach for cell lysis and membrane isolation, that will allow differential separation of inner and outer membranes using sucrose density centrifugation. Development of such an approach, applied to vegetative and developing cells, will provide a global framework for understanding molecular dynamics leading to *M. xanthus* development. Specifically, development of such a technique will have a major impact on models of C-signaling. According to one model, CsgA is associated with the inner membrane, where it acts as an enzyme generating a product that is the actual C-signal. In this model C-signal, a small molecular weight molecule, is secreted where it signals other cells. Whereas this model predicts that CsgA remains associated with the inner membrane throughout its life cycle, the second model argues that the C-signal is the proteolytically cleaved, 17-kDa protein form, which localizes to the outer membrane. This study focuses on membrane separation of vegetative, wild-type *M. xanthus* DK1622 cells and reports localization of several outer surface proteins including CsgA.

CHAPTER 2

MATERIALS AND METHODS

Bacterial strains and reagents. Wild-type *Myxococcus xanthus* strain DK1622 was used in all experiments. DK1622 was grown in casitone yeast extract medium (CYE) containing 1% casitone (Difco), 0.5% yeast extract (Difco), 10 mM 4-morpholinepropanesulfonic acid (MOPS) buffer, pH 7.6, and 0.1% $MgSO_4$. Cells were grown in a 2-L flask containing 1200 ml CYE to an optical density of 0.15-02 A_{550} or 2 $x10^8$ cells/ml. Sucrose solutions were made in 20 mM N-2-hydroxyethylpiperazine-N'-2-ethanesulfonic acid (Hepes) with 5 mM ethylenediaminotetracetic acid (EDTA), pH 7.6 (HE5), or in 20 mM Hepes, pH 7.6 buffer (HE). Membrane enrichments were diluted in 20 mM Hepes/ 0.1 mM EDTA, pH 7.6 (HE0.1). The density of each sucrose solution was determined at room temperature using a refractometer. Sucrose solutions were stored at 4°C and mixed before use.

Membrane separation. This technique is a combination of methods developed by Orndorff (84) and Kotarski and Salyers (56). 1200 ml cultures of DK1622 grown to midlog phase (about 2 $x10^8$ cells/ml), were split into 300 ml aliquots, mixed with 100 ml of ice-cold double distilled water and collected by centrifugation at 10,000 x g for 10 minutes. The cells were washed with 100 ml of ice cold distilled water and centrifuged at 10,000 x g for 10 minutes. The washed cell pellet was resuspended in 10 volumes (approximately 40-50 ml) of 23.5% sucrose in HE buffer and the suspension was transferred to a 250 ml beaker. Freshly prepared chicken egg white lysozyme (Sigma)

(0.12 mg/ml in water) and 100 mM EDTA in water, pH 7.6 were added to a final concentration of 300 μg/ml and 1 mM respectively. The cell suspension was incubated at 4°C with gentle stirring for 14-16 hours. The next day, lysozyme-EDTA-treated cells were distributed in four 50 ml tubes and collected at 27,000 x g for 15 minutes. The pellets were resuspended by pipetting in 2 volumes of ice-cold doubly distilled (dd) water. The rest of the pellet was resuspended by the addition of the third volume (approximately 6 ml of total volume).

Spheroplasting cells were transferred to a 30 ml beaker and stirred for 30 minutes. Conversion of osmotically shocked cells into circular spheroplasts was monitored microscopically. Spheroplasts were collected by centrifugation at 12,000 x g for 10 minutes. The supernatant was reserved while the pellet was resuspended in 3 volumes of 5 mM EDTA, pH 7.6. One tablet of Complete EDTA-free protease inhibitor (Roche) was dissolved and the suspension was stirred for 1 hour. After this time, the supernatant was added back to the suspension and stirred for 30 minutes. Finally, 10 mg of RNaseA (Sigma) and 10 mg DNase type II (Sigma), previously suspended in 1 ml of double distilled water each, were added and incubated for an additional 30 minutes. This suspension was placed in two 50 ml Falcon tubes and diluted 4-fold in HE0.1 buffer. Intact cells were separated from the spheroplasts by several 10 minute centrifugations at 5,000 x g. Spheroplasts were removed from intact cells by resuspension using a Pasteur pipette.

The final suspension was aliquoted into 12 tubes and the membranes were collected by ultracentrifugation for 2 hours at 100,000 x g in a Ti 70.1 rotor (Beckman). Each membrane pellet was gradually resuspended in 0.5 ml aliquots of 23.5% sucrose in HE5 buffer using a Dual 21 tissue homogenizer (Kontes). Membranes were ground using vertical and circular strokes with minimal introduction of air bubbles. 12.4 ml of the total membrane material was incubated overnight with gentle stirring. The next day, 1 tablet of

Complete EDTA-free protease inhibitor was added. 0.4 ml of the membrane suspension was stored at 4°C as a control for immunoblot and enzyme analysis. The remaining 12 ml were loaded on the top of the four, three-step gradients, each consisting of 10 ml of 60% sucrose, 10 ml of 48% sucrose, and 10 ml of 35% sucrose made in HE5. The membranes were separated in a SW 28 rotor at 120,000 x g for 3 hours.

The material that migrated at the interface of 48% and 35% sucrose layers (light membrane enrichment) was transferred to a new 38 ml centrifuge tube and diluted with HE0.1 to nearly fill the tube. Then, 1 ml of 30% sucrose was placed on the bottom of the tube to create a cushion. The material that migrated at the interface of 35% and 48% sucrose layers (medium density membrane enrichment) was transferred to another tube, diluted with HE0.1 as above, and cushioned with the 40% sucrose. The material that migrated at the interface of 48% and 60% sucrose (heavy membrane enrichment) was diluted with HE0.1 and cushioned with 1 ml of 50% sucrose. Heavy and medium membrane enrichments were collected by ultracentrifugation in a SW28 rotor at 26,000 rpm (120,000 x g) for 3 hours, while the light membrane enrichment was collected for 6 hours. Concentrated enrichments were diluted with 1-3 ml of HE0.1 to reach 20% sucrose (heavy and medium membrane enrichment) and 15% sucrose (light membrane enrichment). A tablet of Complete EDTA-free protease inhibitor was added to each membrane suspension. Because of the large yield, the heavy membrane enrichment was split in two and loaded on two gradients.

Membrane enrichments were layered on top of discontinuous gradients. The heavy membrane gradient consisted of 4 ml of 70% sucrose, 4 ml of 60%, 15 ml of 55%, 3 ml of 40%, and 3 ml of 30% sucrose solutions in HE5. The intermediate membrane enrichment contained 3 ml of 70%, 4 ml of 60%, 4 ml of 55%, 15 ml of 46%, 3 ml of 40%, and 3 ml of 30% sucrose solutions in HE5. The light membrane enrichment contained: 4 ml of 70%, 4 ml of 60%, 4 ml of 55%, 15 ml of 37.5%, 3 ml of 30%, and 3

ml of 20% sucrose in HE5. Gradients were spun at 120,000 x g for 16 hours in SW28 rotor and fractionated into 1 ml aliquots using a gradient fractionator (Hoefer Scientific). Density and relative protein content (A_{280}) were determined for every other fraction using a refractometer (Bausch and Lomb) and a UV-VIS Spectrophotometer (Beckman), respectively. Fractions under each peak were consolidated, diluted to 35 ml of final volume with HE0.1 buffer and centrifuged in a Beckman SW28 rotor for 12-16 hours at 120,000 x g. The washing step was repeated one more time to ensure sucrose removal. Membrane pellets were resuspended in a small volume of HE0.1 buffer using a tissue grinder. Characterization of membrane fractions was performed within 48 hours. During this time 50 µl aliquots of each sample were kept at 4°C while the remaining samples were frozen at -20°C.

Preparation of fraction VII. Cells were grown, collected and incubated in sucrose/lysozyme/EDTA as noted above. Total membranes were collected for 2 hours at 100,000 x g in Ti 70.1 rotor, after which membranes were homogenized using a tissue homogenizer. Following the addition of protease inhibitors, membranes were loaded immediately on a linear sucrose gradient consisting of 5 ml of 60%, 50%, 45%, 40%, 35%, 30%, and 25% sucrose. Gradient ultracentrifugation and fractionation was performed as noted above.

Gel electrophoresis and immunoblotting. Protein concentration was determined using bicinchoninic acid assay (BCA) (Pierce). Depending on the immunoblot, 4-20 µg of each sample were separated on a 15% sodium dodecyl sulfate polyacrylamide gel electrophoresis (SDS-PAGE) (62). Low Range Prestained SDS-PAGE Standards (BioRad) were used for SDS-PAGE gels. Proteins were transferred onto a 45 µm nitrocellulose membrane (BioRad) in a BioRad Trans Blot Cell (80 mA for 5 hours)

using Towbin buffer (114). Membranes were blocked in Tris buffered saline (TBS) buffer containing 5% milk, with the exception of FrzCD, which was blocked in 10% milk (74). For Tgl (93), PilA (127), CsgA (58), and FrzCD immunoblots (74), 4-20 μg of protein/lane was reacted with the corresponding antibody in 1:2000, 1:2000, 1:5000, and 1:500 dilutions respectively. Secondary anti-rabbit antibody conjugated with horseradish peroxidase (HRP) (Cell Signaling) was added at a 1:3000 dilution. For lipid A, O-antigen, and FibA specific immunoblots, 4-10 μg of protein/ lane was reacted with monoclonal antibodies 2254, 783, and 2105 in 1:500, 1:1000, and 1:500 dilutions respectively (24, 28, 29). Secondary goat anti-mouse antibody was used in a 1:10,000 dilution. Reactive bands were visualized using the ECL reagents (Amersham Pharmacia, Inc) and recorded on Hyperfilm (Amersham Pharmacia Biotech). Reactive bands were quantified using Scion Image software (Scion Corporation).

Enzyme assays and biochemical analysis. The succinate dehydrogenase assay was performed according to Kasahara and Anraku (49) with the following modifications: assays were done using 15 μg instead of 33 μg of protein, and sarkosyl was added to a final concentration of 0.25%. The reaction mixture was equilibrated for 2 minutes before addition of membrane protein. After 3 minutes of incubation, 2,6-dichlorophenolindophenol (DCPIP) (Fluka) and phenazine methosulfate (PMS) were added. Decrease in absorption at 600 nm was recorded after 3 minutes.

Protein fingerprinting and sequence analysis. For protein fingerprinting 25 μg of protein was separated on a 7.5% polyacrylamide gel and stained with Coomassie blue R 250 for 2 hours. The five most intense protein bands were excised and frozen in 1% acetic acid. Gel slices were digested with trypsin and analyzed by matrix-assisted laser desorption ionization time of flight mass spectroscopy (MALDI TOF MS). Since

fingerprinting data did not yield strong hits with any protein in the public database, the fingerprinting data were sent to Cereon LLT where the matching gene in the *M. xanthus* genome database was found.

2D SDS-PAGE analysis. Two-dimensional electrophoresis was performed according to the method of O'Farell (83) by Kendrick Labs, Inc (Madison, WI). Isoelectric focusing was carried out in glass tubes of inner diameter 2.0 mm using 2% pH 3.5-10 ampholines (Gallard Schlesinger Industries) for 9600 volt-hrs. 100 μg of protein was equilibrated in 10% glycerol, 50 mM dithiothreitol, 2.3% SDS, and 0.0625 M Tris, pH 6.8 for 10 minutes. Carbamylated carbonic anhydrase markers were added to each sample. The isoelectric points of each of the charged forms in 9 M urea at room temperature measured: spot 1- 7.3 ± 0.05, spot 2- 7.11 ± 0.03, spot 3- 6.97 ± 0.02, spot 4- 6.75 ± 0.02, spot 5- 6.61 ± 0.01, spot 6- 6.45 ± 0.04, spot 7- 6.27 ± 0.04, spot 8 ± 6.11 ± 0.05, spot 9- 6.01 ± 0.04, spot 10- 5.86 ± 0.04, spot 11- 5.7 ± 0.03, spot 12- 5.63 ± 0.03, spot 13- 5.54 ± 0.02, spot 14- 5.46 ± 0.02, spot 15- 5.37 ± 0.02, spot 16- 5.27 ± 0.02, spot 17- 5.2 ± 0.02, spot 18- 5.14 ± 0.02, spot 19- 5.08 ± 0.02, and spot 20- 4.99 ± 0.03. Each tube was sealed to the top of a stacking gel. SDS slab gel electrophoresis was carried out on 10% acrylamide gel (0.75 mm thickness) for 4 hours at 15 mA. Gels were stained in Sypro Ruby stain (Biorad) and imaged using Typhoon 9400 Variable Mode Imager (Applied Biosystems).

CHAPTER 3

RESULTS

Vegetative DK1622 cells were incubated overnight in 23% sucrose containing lysozyme (0.3 mg/ml) and 1 mM EDTA, then osmotically shocked with water to form spheroplasts. Total membranes were separated from soluble material by ultracentrifugation (100,000 x g, 2 hours), then subjected to mechanical grinding using a tissue homogenizer, followed by an overnight incubation in 23% sucrose containing 5 mM EDTA. Membranes prepared in this manner were subsequently applied to a three-step sucrose gradient (Figure 3.1 A). Three bands were observed; each was concentrated, then separated on a discontinuous sucrose gradient. The preparation yielded seven membrane fractions (Figure 3.2).

Biochemical characterization of the isolated membrane fractions. Biochemical markers were used to determine the identity of the isolated membrane fractions, and the extent of their contamination. Succinate dehydrogenase (SDH) was used as an inner membrane marker (49), while monoclonal antibody 2254, specific to the lipid A portion of lipopolysaccharide (LPS), was the outer membrane marker (24). Lipid A produces a compact band on upon SDS-PAGE convenient for quantification. Membrane markers were quantified for each fraction and are given as the percent of a marker recovered in the fraction divided by the total marker recovered from all fractions.

Peak I, with a density of 1.292-1.310 g/ml, contained about 25% of the total SDH activity and 16% of the total lipid A (Table 3.1). After collection by ultracentrifugation, peak I had a brownish appearance, and showed a strong tendency to agglutinate after resuspension in buffer. Peak II contained 11% of total SDH and 8% of the lipidA. Peak III was isolated in low abundance and was not characterized (Figure 3.2). Peak IV, with a density of 1.197 g/ml, formed a yellow, sticky pellet resembling that of the total membrane. On average, peak IV contained 62% of the total SDH and 48% of the lipid A. Peaks V and VI together contained 2% of the total SDH activity and about 27% of the total lipid A. Peak V formed a thin, whitish band with a peak density of 1.213-1.229 g/ml, while fraction VI was yellow with a density of 1.169-1.171 g/ml. However, after collection, both peaks V and VI were distinctly yellow, except that peak VI appeared more translucent. Peaks V and VI were easy to resuspend and did not fall out of the suspension. A puzzling observation was that peaks IV and V, which had very different biochemical properties, displayed similar buoyant densities (1.197 vs. 1.220 g/ml). Based on the distribution of membrane markers, and their buoyant densities, we suggest that peak I corresponds to the inner membrane, peak II and IV correspond to hybrids of inner and outer membrane, and peaks V and VI correspond to outer membrane fractions.

Inner membrane contained 42% of the total membrane protein. The second most protein-rich peak was peak IV (32%), which contained the majority of both inner and outer membrane markers (Table 3.1). Outer membrane peaks V and VI together contained only 10% of total membrane protein. The low percentage of total SDH activity recovered from the peak I appeared to be the result of a non-uniform distribution of SDH across the inner membrane, as 3-fold higher SDH specific activity was present in peak IV. Inner membrane contains more lipid A than the outer membrane contains SDH, which is to be expected as lipid A is synthesized in the inner membrane. The overall

recovery of succinate dehydrogenase was 74 ± 9 %, and overall protein recovery was 50.66 ± 4.6 %.

Immunoblot analysis of membrane fractions. Membrane peaks were probed with antibodies against well known antigens (Figure 3.3). Identical amounts of protein were loaded in each lane and the gel was subjected to Western analysis. Lipid A, which was used as the outer membrane marker, was found predominantly in peak IV and peaks V and VI, reaching the highest concentration (amount of lipid A/ mg protein) in peak V (Figure 3.3 A). Monoclonal antibody 783, specific to LPS O-antigen, followed a similar pattern, reaching the maximum concentration in peak VI (Figure 3.3 B). Tgl is a putative outer membrane protein that contains a 19 amino acid N-terminal signal sequence common to lipoproteins (93). Tgl is required for assembly of type IV pili (tfp), which are necessary for social motility. Tgl antibody reacted strongly with both outer membrane peaks V and VI, while 20-fold and 10-fold lower levels of Tgl were detected in peaks I and IV respectively (Figure 3.3 C).

PilA is the structural protein for type four pili, which are found exclusively on the cell poles (47, 126). Prepilin monomers should reside in the inner membrane and become assembled after N-terminal signal cleavage and methylation via a type II secretion mechanism (70). Accordingly, prepilin and pilin PilA forms of *M. xanthus* should yield 25- and 23-kDa protein forms based on predicted amino acid sequence. While the presence of prepilin could not be detected, two major bands of 29- and 26-kDa were found distributed in different amounts in all membrane fractions (Figure 3.3 D). Both forms represent mature pilin as they were detected in pili sheared from intact cells (119). In addition, two smaller bands were present in amounts proportional to the 29- and 26-kDa antigens and are most likely pilin degradation products. Approximately similar levels of PilA were found in peaks I, V, and VI, while the hybrid membrane peaks II and IV showed a two-fold enrichment.

Inner membrane, and to a lesser degree peak II vesicles, agglutinated rapidly and were reminiscent of behavior of intact cells during a cohesion assay. Cell cohesion is a consequence of the adhesive nature of fibrils. Although the molecular mechanism of cohesion is unknown, a monoclonal antibody exists to FibA, a fibril-associated protein (5). FibA is associated with extracellular matrix during starvation and is a member of the M4 zinc-dependent metalloprotease family (50). Whereas only a 68-kDa form is detected in vegetative cells grown in a liquid CYE medium (data not shown), at least 3 processed forms are found in cells grown at high density on a nutrient rich CTT agar (50), or starved in agglutination buffer (5). FibA was found exclusively associated with the inner membrane and peak II (Figure 3.3 E). It was peculiar to find the processed 32-kDa form also present, which might suggest physiological changes during overnight incubation in sucrose/lysozyme/EDTA solution. Despite the high concentration of cells in this solution, constant stirring should have minimized intercellular contacts. This leads to the conclusion that fibril synthesis might be induced via the starvation-dependent pathway.

CsgA is a C-signal producing protein that is required for development (52, 58, 65). CsgA is present in two protein forms during development: a full-length protein with homology to short chain alcohol dehydrogenases (25-kDa) (63) and a processed 17-kDa form (53, 58). The nature of the C-signal is controversial as it remains unclear whether 17-kDa form of CsgA acts directly as a protein signal, or whether the signal is an as yet unknown enzymatic product of 25-kDa CsgA. Whereas the first model envisions CsgA cleavage and export to the outer membrane, the latter model predicts CsgA as part of the inner membrane electron transport network. In this sense, CsgA localization might aid in our understanding of C-signal generation. The full- length protein localizes to the inner membrane, while a small amount of full-length protein is present in membrane fusions

and outer membranes (Figure 3.3 F). The short form, which is present in 10-fold lower amounts, could not be localized in vegetative cells.

FrzCD is essential for fruiting body morphogenesis, and regulates cell reversal (8, 132). FrzCD is a homologue of *E. coli* methyl-accepting chemotaxis proteins (MCP) (72). Generally, MCP proteins have transmembrane topology with a characteristic periplasmic domain for ligand binding. Unlike other members of its family, FrzCD lacks the membrane-spanning domains (72), although the protein is membrane associated. FrzCD is highest in peak IV, with 1.5-2-fold higher amounts than in the inner membrane. However, it is surprising that FrzCD is also detected in the outer membrane peaks V and VI. Peak VI contained on average 80% of the FrzCD present in the inner membrane. This finding may highlight a novel aspect of FrzCD.

Two dimensional analysis of isolated fractions. To perform a more detailed protein analysis of the four most abundant membrane fractions, 100 μg of each membrane sample was separated on a 2-dimensional SDS polyacrylamide gel. The inner membrane contained a range of different sized acidic proteins that did not resolve well by isoelectric focusing. The intensity of the streaks suggests that they are likely to be major components of the inner membrane proteome (Figure 3.4 A). Manual alignment of inner and outer membrane gels identified 10 spots that were common to both peaks (Figure 3.4 A, indicated with arrows pointing down). Five of these spots were in the molecular weight range between 43 to 29 kDa. In contrast to the inner membrane, neither outer membrane contained large quantities of acidic proteins (Figures 3.4 A, C & D). The two outer membrane proteomes appeared similar, yet differed greatly in the levels of several groups of proteins (Figure 3.4 C and D). Proteins contained in clusters 1, 2, 3, and 5 were barely detectable in peak V relative to peak VI, suggesting that they are specific to peak VI. Only cluster 4 was more abundant in peak V. Peak IV contained acidic inner

membrane proteins (outlined with rectangle, Figure 3.4 C), but also had 21 spots in common with the outer membrane V (Figure 3.4 C, indicated by arrows).

Peak VII contains Ta-1 polyketide synthetase (PKS). Peak VII had no visible color on the gradient and an unusually low buoyant density (1.094-1.072 g/ml) (Figure 3.2 C). Despite high absorbance at 280 nm, yields of peak VII were small compared to the other 6 fractions. However, when the experimental procedure was shortened and the spheroplasted membrane material loaded directly on a linear sucrose gradient, larger amounts were recovered. Peak VII displayed a small set of very intense bands upon SDS-PAGE (Figure 3.5 A). Five peptides of sizes 90 kDa, 86 kDa, 71 kDa, 55 kDa, and 45 kDa were submitted to MALDI-TOF mass spectroscopy fingerprinting analysis following trypsin digestion. Since this strategy did not yield any significant hits against the proteins in the database, the *M. xanthus* genome sequence was examined to match the fingerprinting data against *M. xanthus* proteome. Surprisingly, all five proteins are processed products of polypeptide MYX12U-3797, which is predicted to be 7,831 amino acids in length. A portion of MYX12U-3797 was found in GenBank as *M. xanthus* TA-1 polyketide synthatase (PKS), which had 99% amino acid identity over 2392 amino acids (85).

Ta-1 has combined structural elements of a non-ribosomal peptide synthetase (NRPS), and a type I polyketide synthetase (85) (Figure 5 B). While NRPS assemble products by covalently linking amino acids (131), type I PKS assemble products through incorporation of acyl extender units. Ta-1 exhibits modular organization similar to type I PKS, common to animal and yeast fatty acid synthetases (108). In a type I PKS mechanism, each module is responsible for covalent addition, and sometimes reduction, of an acetate or propionate extender unit into the elongating chain. Ta-1 is a member of a large PKS cluster of genes originally discovered in *M. xanthus* strain TA isolated in Tel

Aviv. The TA cluster was reported to encode antibiotic TA (94), also known as myxovirescin A (115), whose structure has been elucidated.

Analysis of Ta-1 conserved domains, performed using the conserved domains search program (1), indicates that the first 1000 amino acids in the amino terminus comprise a loading domain, which consists of a condensation domain (C), an amino acid activation domain (A), and an acyl carrier protein group (ACP) (Figure 5 B). The condensation domain performs peptide bond formation in non-ribosomal peptide biosynthesis. Downstream of the condensation domain is the amino acid activation domain, also known as the adenylation domain (A), which is responsible for amino acid activation as an adenylate intermediate at the expense of ATP. The activated amino acid/acyl extender unit is sequentially transferred to the thiol residue of a peptydyl/acyl carrier protein PCP/ ACP domain. PCP/ACP, which acts as a swinging arm will transfer the thiol derivative to the KS domain of the first chain extension module.

The amino acid activation domain of Ta-1 contains all five conserved motifs (131) with the following sequence conservation: motif A (L_AG_AYVP), motif B (Y_SGTTGxPKGV), motif C (GEL_IGGXGxARGYL), motif D (YxTGD), and motif E (VK_ RGxRIE_GEIE), where x indicates any amino acid. Underlined spaces indicate discrepancies with the published motifs. Motifs B, C, D, and E are engaged in ATP binding and formation of amino acid adenylate (32, 87, 88, 118). Analysis of other peptide synthetases has indicated that each activation domain is responsible for activation of a single amino acid. Modules 1, 2, and 4 are organized as typical type I PKS modules consisting of β-keto synthase/acyltransferase (KS/AT) and acyl carrier protein (ACP) chain elongation units, and β-keto-reductase (KR) reducing unit. However, modules 3 and 5 lack KR units. The lack of reductive domains in PKS modules is not unusual (108) and contributes to the structural variation in natural products. Finally, the sixth module

consists of only the KS/AT domain, suggesting that Ta-1 is a part of a larger biosynthetic cluster.

CHAPTER 4

DISCUSSION

This is the first study that reports the membrane separation and characterization of wild-type *M. xanthus* strain DK1622. Initial preparation of cells is similar to the procedure of Orndorff for mutant MD-2 (84). Conversion of vegetative cells to spheroplasts required overnight exposure to lysozyme and EDTA. Even under these conditions spheroplasting was only 80-90% efficient and removal of unlysed cells was required. To achieve membrane separation, it was necessary to grind membranes with a tissue homogenizer and subject them to additional overnight incubation. Reproducibility of the separation technique was dependent on three factors: the volume of water used for spheroplasting, the volume of 5 mM EDTA added during subsequent incubation of spheroplasts, and the manner in which homogenization was performed. To provide adequate and uniform shearing, the total membrane had to be centrifuged in 7-8 ml increments in a Ti 70.1 rotor to produce smaller pellets. These pellets were then gradually resuspended and ground in 0.5 ml aliquots of 23% sucrose. Collection of membranes in the SW28 rotor produced larger pellets that could not be uniformly homogenized, which resulted in unpredictable protein elution profiles from the discontinuous gradients. A factor that had a deleterious effect on membrane separation was the presence of calcium cations, which caused clumping of the cells. Separation of cell membranes grown under these conditions yielded a broad hybrid peak at 1.197 g/ml. Problems with calcium were due to detergent residuals and were eliminated by extensive washing of glassware with distilled water.

Besides the above mentioned parameters required for membrane preparation, another crucial element was design of the sucrose gradients. In this regard, introduction of a three-step gradient as the initial step in separation was essential to provide physical separation of outer membranes from hybrid membrane (peak IV) even though these two fractions have almost identical densities (1.197 vs. 1.220 g/ml).

In comparison with the previous work on membrane separation of mutant MD-2 (84), the density of outer membrane (peak VI) is similar to the single outer membrane peak of MD-2 mutant (1. 170 vs. 1.166 g/ml). The hybrid membrane (peak IV) appears as a heavier counterpart of Orndorff's hybrid membrane (1.197 vs. 1.185 g/ml), while the buoyant density difference between inner membranes of DK1622 and MD-2 strain is the largest (1.30 vs. 1.22 g/ml). Besides the differences in buoyant densities, the hybrid membranes of the two strains had different SDH specific activities. Also, the outer membrane of MD-2 strain eluted as a single band whereas that of DK1622 eluted as two peaks. The differences in buoyant densities of inner membranes might be due to different physical treatments of membranes (i.e. syringe versus a tissue homogenizer).

The most unusual fraction isolated in this procedure was the hybrid membrane peak IV which was highly enriched in both lipid A and SDH. Large hybrid peaks are not unusual for this type of procedure (9, 56). Since electron microscopy (EM) failed to reveal any junctions or fusions between the membranes (117), it seems likely that the membranes are held together through protein interactions. This might be due to the unusual structure of *M. xanthus* cell wall, much of which is made of nonpeptidoglycan material, assumed to consist of lipids and proteins rich in glycine (123). Initial characterization of peak IV by Western blot analysis revealed a two-fold enrichment of PilA and FrzCD proteins compared to the inner membrane. Higher levels of PilA might suggest that this fraction includes cell poles where the pilus motor is located. Tighter

coupling between the two membranes might play a specialized function in tfp biogenesis by facilitating assembly and export of tfp to the surface.

Fraction VII had very low levels of SDH, while the amounts of measured lipid A were similar to the levels found in the total membrane (data not shown). Myxovirescin A (TA) is produced during exponential growth and purified from the culture supernatant (27). TA inhibits cell wall synthesis of gram-type negative bacteria (130). A study by Gerth and co-workers demonstrated that *Myxococus virescens* displays greater sensitivity to TA than *E. coli*, with the minimum inhibitory zone being 1 μg/ml for *E. coli* and 0.5 μg/ml for *M. virescens* (27). *P. aeruginosa* required as much as 30 μg/ml of TA antibiotic to inhibit cell growth. Therefore, the finding that the polyketide synthetase responsible for TA production co-localizes with the membranes where it could inhibit peptidoglycan synthesis is intriguing. Membrane localization of TA-1 PKS may provide an explanation as to how *M. xanthus* expedites secretion of a metabolite inhibitory to its own growth. It is possible that the cell encloses TA biosynthetic machinery into phospholipid vesicles or cages to protect the peptidoglycan. This hypothesis is in agreement with previous experiments indicating inhibition of TA activity by phospholipids and cholesterol (27).

The inner and outer membrane proteomes appear to cluster in specific pI ranges. The inner membrane proteome contains a bimodal distribution of proteins as a function of pI with greatest abundance in the 3.5-4.0 and the 5.0-7.0 pI ranges. The outer membrane proteome displays a unimodal protein distribution in the 5-7 pI range. Among the few published 2D gel analyses of outer membrane proteomes, the outer membrane of *E. coli* follows the same trend (77), while *C. crescentus* outer membrane proteins are found predominantly in 8-11 pI range (78). As we are still in the early stages of proteome analysis, it is not known how general this trend is, and if it has any biological repercussions on pathways for protein transport and localization.

MCP proteins of *E. coli* and *C. crescenthus* are inner membrane proteins found localized to the cell poles, where they play a sensory role in chemotactic behavior (69). An unexpected finding of this study was localization of FrzCD, a MCP homologue, in the outer membranes. Since both outer membrane peaks contain low levels of succinate dehydrogenase, contamination is not a likely explanation for observed results. Such a requirement can be explained with different domain organization of FrzCD as well as with the more complex functions this protein plays in perception of stimuli and control of motility. FrzCD lacks transmembrane and periplasmic, ligand-binding domains (72). In addition, FrzCD responds to remarkable number of stimuli, including saturated fatty acids, alcohols, lipoic acid (73), Tgl (119), and C-signal (107). It is plausible that sensing and integrating such a large number of stimuli requires separation (specialization) of function through dual localization in both inner and outer membranes. According to this model, a certain number of stimuli, such as those offered by Tgl, or Cgl lipoproteins can only be perceived through the direct contact and require FrzCD-protein interaction. FrzCD localized in the outer membrane may perceive stimuli directly via protein-protein interactions, while in the inner membrane it senses smaller compounds (lipids, alcohols) that can enter the cell.

The outcome of the CsgA localization experiment supports our prediction that CsgA acts as an enzyme from the inner membrane. However, to critically evaluate the two models, localization of the minor, and proteolitically cleaved protein needs to be performed. This will require examining protein localization in cells undergoing development since the small form is difficult to detect during vegetative growth.

REFERENCES

1. **Altschul, S.F., Madden, T.L., Schaffer, A.A., Zhang, J., Zhang, Z., Miller, W., and Lipman, D.J.** (1997) Gapped BLAST and PSI-BLAST: a new generation of protein database search programs. *Nucleic Acids Res.* **25**: 3389-3402.

2. **Arnold, J.W., and Shimkets, L.J.** (1988) Cell surface properties correlated with cohesion in *Myxococcus xanthus*. *J. Bacteriol.* **170**: 5771-5777.

3. **Baker, M.** (1994) *Myxococcus xanthus* C-factor, a morphogenetic paracrin signal, is similar to *Escherichia coli* 3-oxoacyl-[acyl-carrier-protein] reductase and human 17ß-hydroxysteroid dehydrogenase. *Biochem. J.* **301**: 311-312.

4. **Behmlander, R., and Dworkin, M.** (1994) Biochemical and structural analyses of the extracellular matrix fibrils of *Myxococcus xanthus*. *J. Bacteriol.* **176**: 6295-6303.

5. **Behmlander, R.M., and Dworkin, M.** (1991) Extracellular fibrils and contact-mediated cell interactions in *Myxococcus xanthus*. *J. Bacteriol.* **173**: 7810-7821.

6. **Beveridge, T.J.** Unpublished data.

7. **Beveridge, T.J.** (1999) Structures of gram-negative cell walls and their derived membrane vesicles. *J. Bacteriol.* **181**: 4725-4733.

8. **Blackhart, B.D., and Zusman, D.R.** (1985) Frizzy genes of *Myxococcus xanthus* are involved in control of frequency of reversal of gliding motility. *Proc. Natl. Acad. Sci. USA* **82**: 8767-8770.

9. **Bledsoe, H.A., Carroll, J.A., Whelchel, T.R., Farmer, M.A., Dorward, D.W., and Gherardini, F.C.** (1994) Isolation and characterization of *Borrelia*

burgorferi inner and outer membranes by using iospycnic centrifugation. *J. Bacteriol.* **176**: 7447-7455.

10. **Bowden, M.G., and Kaplan, H.B.** (1998) The *Myxococcus xanthus* lipopolysaccharide O-antigen is required for social motility and multicellular development. *Molec. Microbiol.* **30**: 275-284.

11. **Boysen, A., Ellehauge, E., Julien, B., and Sogaard-Andersen, L.** (2002) The DevT protein stimulates synthesis of FruA, a signal transduction protein required for fruiting body morphogenesis in *Myxococcus xanthus*. *J. Bacteriol.* **184**: 1540-1546.

12. **Burnham, J.C., Collart, S.A., and Highison, B.W.** (1981) Entrapment and lysis of the cyanobacterium *Phormidium luridum* by aqueous colonies of *Myxococcus xanthus* PCO2. *Arch. Microbiol.* **129**: 285-294.

13. **Burnham, J.C., Collart, S.A., and Daft, M.J.** (1984) Myxococcal predation of the cyanobacterium *Phormidium luridum* in aqueous environments. *Arch. Microbiol.* **137**: 220-225.

14. **Cashel, M., Gentry, D.R., Hernandez, V.J., and Vinela, D.** (1996) The stringent response. In *Escherichia coli and Salmonella: cellular and molecular biology*. Neidhardt, F.C., III, R.C., Ingraham, J.L., Lin, E.C.C., Low, K.B., Magasanik, B., Reznikoff, W.S., Riley, M., Schaester, M. and Umbarger, H.E. (eds). Washington, D. C.: ASM Press.

15. **Cheng, Y., and Kaiser, D.** (1989) *dsg*, a gene required for *Myxococcus* development, is necessary for cell viability. *J. Bacteriol.* **171**: 3727-3731.

16. **Cho, K., and Zusman, D.R.** (1999) AsgD, a new two component regulator required for A-signaling and nutrient sensing during early development of *Myxococcus xanthus*. *Molec. Microbiol.* **34**: 268-281.

17. **Crawford, J., E. W., and Shimkets, L.J.** (2000) The stringent response in *Myxococcus xanthus* is regulated by SocE and the CsgA C-signaling protein. *Genes Develop.* **14**: 483-492.

18. **Crawford, J., E. W., and Shimkets, L.J.** (2000) The *Myxococcus xanthus socE* and *csgA* genes are regulated by the stringent response. *Molec. Microbiol.* **37**: 788-799.

19. **Dailey, H.A., and Dailey, T.A.** (1996) Protoporphyrinogen oxidase of *Myxococcus xanthus*: expression, purification, and characterization of the cloned enzyme. *J. Biol. Chem.* **271**: 8714-8718.

20. **Davis, J.M., Mayor, J., and Plamann, L.** (1995) A missense mutation in *rpoD* results in an A-signalling defect in M*yxococcus xanthus*. *Molec. Microbiol.* **18**: 943-952.

21. **Dawid, W.** (2000) Biology and global distribution of bacteria in soils. *FEMS Microbiol. Rev.* **24**: 403-427.

22. **Dworkin, M.** (1962) Nutritional requirements for vegetative growth of *Myxococcus xanthus*. *J. Bacteriol.* **84**: 250-257.

23. **Ellehauge, E., Norregaard-Madsen, M., and Sogaard-Andersen, L.** (1998) The FruA signal transduction protein provides a checkpoint for the temporal co-ordination of intercellular signals in *Myxococcus xanthus* development. *Molec. Microbiol.* **30**: 807-817.

24. **Fink, J.M., and Zissler, J.F.** (1989) Characterization of lipopolysaccharide from *Myxococcus xanthus* by use of monoclonal antibodies. *J. Bacteriol.* **171**: 2028-2032.

25. **Fontes, M., and Kaiser, D.** (1999) *Myxococcus* cells respond to elastic forces in their substrate. *Proc. Natl. Acad. Sci. USA* **96**: 8052-8057.

26. **Garza, A.G., Harris, B.Z., Pollack, J.S., and Singer, M.** (2000) The *asgE* locus is required for cell-cell signaling during *Myxococcus xanthus* development. *Mol. Microbiol.* **35**: 812-824.

27. **Gerth, K., Irschik, H., Reichenbach, H., and Trowitzsch, W.** (1982) The myxovirescins, a family of antibiotics from *Myxococcus virescens* (Myxobacterales). *J. Antibiot.* **35**: 1454-1459.

28. **Gill, J., Stellwag, E., and Dworkin, M.** (1985) Monoclonal antibodies against cell-surface antigens of developing cells of *Myxococcus xanthus*. *Ann. Inst. Pasteur/Microbiol.* **136 A**: 11-18.

29. **Gill, J.S., and Dworkin, M.** (1986) Cell surface antigens during submerged development of *Myxococcus xanthus*, as examined with monoclonal antibody probes. *J. Bacteriol.* **168**: 505-511.

30. **Gill, R.E., and Bornemann, M.C.** (1988) Identification and characterization of the *Myxococcus xanthus bsg*A gene product. *J. Bacteriol.* **170**: 5289-5297.

31. **Gill, R.E., Karlok, M., and Benton, D.** (1993) *Myxococcus xanthus* encodes an ATP-dependent protease which is required for developmental gene transcription and intercellular signaling. *J. Bacteriol.* **175**: 4538-4544.

32. **Gocht, M., and Marahiel, M.A.** (1994) Analysis of core sequences in the D-Phe activating domain of the multi-functional peptide synthetase TycA by site-directed mutagenesis. *J. Bacteriol.* **176**: 2654-2662.

33. **Gronewold, T.M., and Kaiser, D.** (2001) The act operon controls the level and time of C-signal production for *Myxococcus xanthus* development. *Mol. Microbiol.* **40**: 744-756.

34. **Guo, D., Bowden, M.G., Pershad, R., and Kaplan, H.B.** (1996) The *Myxococcus xanthus rfbABC* operon encodes an ATP-binding cassette transporter

homolog required for O-antigen biosynthesis and multicellular development. *J. Bacteriol.* **178**: 1631-1639.

35. **Guo, D., Wu, Y., and Kaplan, H.B.** (2000) Identification and characterization of genes required for early *Myxococcus xanthus* developmental gene expression. *J. Bacteriol.* **182**: 4564-4571.

36. **Hagen, T.J., and Shimkets, L.J.** (1990) Nucleotide sequence and transcriptional products of the *csg* locus of *Myxococcus xanthus*. *J. Bacteriol.* **172**: 15-23.

37. **Hager, E., H. Tse, and Gill, R.E.** (2001) Identification and characterization of *spdR* mutations that bypass the BsgA protease-dependent regulation of developmental gene expression in *Myxococcus xanthus*. *Mol. Microbiol.* **39**: 765-780.

38. **Harris, B.Z., Kaiser, D., and Singer, M.** (1998) The guanosine nucleotide (p)ppGpp initiates development and A-factor production in *Myxococcus xanthus*. *Genes Develop.* **12**: 1022-1035.

39. **Hodgkin, J., and Kaiser, D.** (1979) Genetics of gliding motility in *Myxococcus xanthus* (Myxobacterales): Genes controlling movement of single cells. *Mol. Gen. Genet.* **171**: 167-176.

40. **Hodgkin, J., and Kaiser, D.** (1979) Genetics of gliding motility in *Myxococcus xanthus* (Myxobacterales): Two gene systems control movement. *Mol. Gen. Genet.* **171**: 177-191.

41. **Jelsbak, L., and Sogaard-Andersen, L.** (1999) The cell surface-associated intercellular C-signal induces behavioral changes in individual *Myxococcus xanthus* cells during fruiting body morphogenesis. *Proc. Natl. Acad. Sci. USA* **96**: 5031-5036.

42. **Jelsbak, L., and Sogaard-Andersen, L.** (2000) Pattern formation: fruiting body morphogenesis in *Myxococcus xanthus*. *Curr. Opin. Microbiol.* **3**: 637-642.

43. **Jelsbak, L., and Sogaard-Andersen, L.** (2002) Pattern formation of cell surface-associated morphogen in *Myxococcus xanthus*. *Proc. Natl. Acad. Sci USA* **99**: 2032-2037.

44. **Julien, B., and Kaiser, D.** Unpublished results.

45. **Julien, B., and Kaiser, A.D.** (2000) Spatial control of cell differentiation in *Myxococcus xanthus*. *Proc. Natl. Acad. Sci. USA* **97**: 9098-9103.

46. **Kadurugamuwa, J.L., and Beveridge, T.J.** (1999) Membrane vesicles derived from *Pseudomonas aeruginosa* and *Shigella flexneri* can be integrated into the surfaces of other Gram-negative bacteria. *Microbiol.* **145**: 2051-2060.

47. **Kaiser, D.** (1979) Social gliding is correlated with the presence of pili in *Myxococcus xanthus*. *Proc. Natl. Acad. Sci. USA* **76**: 5952-5956.

48. **Kalman, L.V., Y. L. Cheng, and Kaiser, D.** (1994) The *Myxococcus xanthus dsg* gene product performs functions of translation initiation factor IF3 in vivo. *J. Bacteriol.* **176**: 1434-1442.

49. **Kasahara, M., and Anraku, Y.** (1974) Succinate dehydrogenase of *Escherichia coli* membrane vesicles. Activation and properties of the enzyme. *J. Biochem (Tokyo)* **76**: 959-966.

50. **Kearns, D.B., Bonner, P.J., Smith, D.R., and Shimkets, L.J.** (2002) An extracellular matrix-associated zinc metalloprotease is required for dilauroyl phosphatidylethanolamine chemotactic excitation in *Myxococcus xanthus*. *J. Bacteriol.* **184**: 1678-1684.

51. **Keseler, I.M., and Kaiser, D.** (1995) An early A-signal-dependent gene in *Myxococcus xanthus* has a σ^{54}-like promoter. *J. Bacteriol.* **177**: 4638-4644.

52. **Kim, S., and Kaiser, D.** (1991) C-Factor has distinct aggregation and sporulation thresholds during *Myxococcus* development. *J. Bacteriol.* **173**: 1722-1728.

53. **Kim, S.K., and Kaiser, D.** (1990) Purification and properties of *Myxococcus xanthus* C-factor, an intercellular signalling protein. *Proc. Natl. Acad. Sci. USA* **87**: 3635-3639.

54. **Kim, S.K., and Kaiser, D.** (1990) Cell motility is required for the transmission of C-factor, an intercellular signal that coordinates fruiting body morphogenesis of *Myxococcus xanthus*. *Genes Develop.* **4**: 896-905.

55. **Kim, S.K., and Kaiser, D.** (1990) Cell alignment required in differentiation of *M. xanthus*. *Science* **249**: 926-928.

56. **Kotarski, S.F., and Salyers, A.A.** (1984) Isolation and Characterization of Outer Membranes of *Bacterioides thetaiotaomicron* Grown on Different Carbohydrates. *J. Bacteriol.* **158**: 102-109.

57. **Kroos, L., Kuspa, A., and Kaiser, D.** (1986) A global analysis of developmentally regulated genes in *Myxococcus xanthus*. *Devel. Biol.* **117**: 252-266.

58. **Kruse, T., Lobedanz, S., Berthelsen, N.M.S., and Sogaard-Andersen, L.** (2001) C-signal: a cell surface-associated morphogen that induces and co-ordinates multicellular fruiting body morphogenesis and sporulation in *Myxococcus xanthus*. *Mol. Microbiol.* **40**: 156-168.

59. **Kuspa, A., Plamann, L., and Kaiser, D.** (1992) Identification of heat-stable A-factor from *Myxococcus xanthus*. *J. Bacteriol.* **174**: 3319-3326.

60. **Lam, H.-M., and Winkler, M.E.** (1992) Characterization of the complex *pdxH-tyrS* operon of *Escherichia coli* K12 and pleiotrophic phenotypes caused by *pdxH* insertion mutations. *J. Bacteriol.* **174**: 6033-6045.

61. **Lancero, H., Brofft, J.E., Downard, J., Birren, B.W., Nusbaum, C., Naylor, J., Shi, W., and Shimkets, L.J.** (2002) Mapping of the *Myxococcus xanthus* social motility *dsp* mutations to the *dif* genes. *J. Bacteriol.* **in press**.

62. **Leammli, U.K.** (1970) Cleavage of strucutural proteins during the assembly of the head of bacteriophage T4. *Nature* **227**: 680-685.

63. **Lee, B.-U., Lee, K., Mendez, J., and Shimkets, L.J.** (1995) A tactile sensory system of *Myxococcus xanthus* involves an extracellular NAD(P)$^+$-containing protein. *Genes Develop.* **9**: 2964-2973.

64. **Lee, K., and Shimkets, L.J.** (1996) Suppression of a signaling defect during *Myxococcus xanthus* development. *J. Bacteriol.* **178**: 977-984.

65. **Li, S., Lee, B., and Shimkets, L.J.** (1992) *csgA* expression entrains *Myxococcus xanthus* development. *Genes Develop.* **6**: 401-410.

66. **Lunsdorf, H., and Reichenbach, H.** (1989) Ultrastructural details of the gliding motility of *Myxococcus fulvus* (Myxobacterales). *J. Gen. Microbiol.* **135**: 1633-1641.

67. **Lunsdorf, H., and Schairer, H.U.** (2001) Frozen motion of gliding bacteria outlines inherent features of the motility apparatus. *Microbiology* **147**: 939-947.

68. **MacNeil, S.D., Calara, F., and Hartzell, P.L.** (1994) New clusters of genes required for gliding motility in *Myxococcus xanthus*. *Molec. Microbiol.* **14**: 61-71.

69. **Maddock, J.R., and Shapiro, L.** (1993) Polar localization of the chemoreceptor complex in the Escherichia coli cell. *Science* **259**: 1717-1723.

70. **Mattick, J.S., Whitchurch, C.B., and Alm, R.A.** (1996) The molecular genetics of type-4 fimbriae in Pseudomonas aeruginosa- a review. *Gene* **179**: 147-155.

71. **McBride, M.** (2001) Bacterial Gliding Motility: Multiple Mechanisms for Cell Movement. *Annu. Rev. Microbiol.* **55**: 49-75.

72. **McBride, M.J., Weinberg, R.A., and Zusman, D.R.** (1989) "Frizzy" aggregation genes of the gliding bacterium *Myxococcus xanthus* show sequence similarities to the chemotaxis genes of enteric bacteria. *Proc. Natl. Acad. Sci. USA* **86**: 424-428.

73. **McBride, M.J., Kohler, T., and Zusman, D.R.** (1992) Methylation of FrzCD, a methyl-accepting taxis protein of *Myxococcus xanthus,* is correlated with factors affecting cell behavior. *J. Bacteriol.* **174**: 4246-4257.

74. **McCleary, W., McBride, M., and Zusman, D.** (1990) Developmental sensory transduction in *M. xanthus* involves methylation and demethylation of FrzCD. *J. Bacteriol.* **172**: 4877-4887.

75. **McCurdy, H.D.** (1989) Fruiting gliding bacteria: The myxobacteria. In *Bergey's Manual*. Vol. 3. Staley, J.T., Bryant, M.P., Pfennig, N. and Holt, J.G. (eds). Baltimore: Williams and Wilkins, pp. 2139-2170.

76. **Merz, A., M. So, and Sheetz, M.P.** (2000) Pilus retraction powers bacterial twitching motility. *Nature* **407**: 98-101.

77. **Molloy, M.P., Herbert, B.R., Slade, M.B., Rabilloud, T., Nouwens, A.S., Williams, K.L., and Gooley, A.A.** (2000) Proteomic analysis of the Escherichia coli outer membrane. *Eur. J. Biochem.* **267**.

78. **Molloy, M.P., Phadke, N.D., Chen, H., Tyldesley, R., Garfin, D.E., Maddock, J.R., and Andrews, P.C.** (2002) Profiling the alkaline membrane proteome of Caulobacter crescentus with two-dimentional electrophoresis and mass spectroscopy. *Proteomics* **2**: 899-910.

79. **Morrison, C.E., and Zusman, D.R.** (1979) *Myxococcus xanthus* mutants with temperature-sensitive, stage-specific defects: evidence for independent pathways in development. *J. Bacteriol.* **140**: 1036-1042.

80. **O' Connor, K.** Unpublished data.

81. **O'Connor, K., and Zusman, D.** (1991) Development in *Myxococcus xanthus* involves differentiation into two cell types, peripheral rods and spores. *J. Bacteriol.* **173**: 3318-3333.

82. **O'Connor, K., and Zusman, D.** (1991) Behavior of peripheral rods and their role in the life cycle of *Myxococcus xanthus*. *J. Bacteriol.* **173**: 3342-3355.

83. **O'Farrell, P.Z., Goodman, H.M., and O'Farrell, P.H.** (1977) High resolution two-dimensional electrophoresis of basic as well as acidic proteins. *Cell* **2**: 1133-1142.

84. **Orndorff, P.E., and Dworkin, M.** (1980) Separation and properties of the cytoplasmic and outer membranes of vegetative cells of *Myxococcus xanthus*. *J. Bacteriol.* **141**: 914-927.

85. **Paitan, Y., G. Alon, E. Orr, E. Z. Ron, and Rosenberg, E.** (1998) The first gene in the biosynthesis of the polyketide antibiotic TA of *Myxococcus xanthus* codes for a unique PKS module coupled to a peptide synthetase. *J. Mol. Biol.* **286**: 465-474.

86. **Parkinson, J.S., and Kofoid, E.C.** (1992) Communication modules in bacterial signaling proteins. *Annu. Rev. Genet.* **26**: 71-112.

87. **Pavela- Vrancic, M., Pfeifer, E., van Liempt, H., Schafer, H.J., von Dohren, H., and Kleinkauf, H.** (1994a) ATP-binding in peptide synthatases: determination of contact sites of the adenine moiety by photoaffinity labelling of tyrocidine synthetase I with 2- azido- adenosine triphosphate. *Biochemistry* **33**: 6276- 6283.

88. **Pavela- Vrancic, M., Pfeifer, E., Schroder, W., von Dohren, H., and Kleinkauf, H.** (1994b) Identification of ATP-binding site in tyrocidine synthetase I by selective modification with fluorescein 5'- isothiocynate. *J. Biol. Chem.* **269**: 14962- 14966.

89. **Plamann, L., Li, Y., Cantwell, B., and Mayor, J.** (1995) The *Myxococcus xanthus asgA* gene encodes a novel signal transduction protein required for multicellular development. *J. Bacteriol.* **177**: 2014-2020.

90. **Plamann, L., and Kaplan, H.** (1999) Cell-density sensing during early development in *Myxococcus xanthus*. In *Cell-cell signaling in bacteria*. Dunny, G.M. and Winans, S.C. (eds). Washington, D. C.: American Society for Microbiology.

91. **Reichenbach, H.** (1993) Biology of Myxobacteria: Ecology and Taxonomy. In *Myxobacteria II*. Dworkin, M. and Kaiser, D. (eds). Washinton DC: American Society for Microbiology, pp. 13-62.

92. **Rodriguez, A.M., and Spormann, A.M.** (1999) Genetic and molecular analysis of *cglB*, a gene essential for single-cell gliding in *Myxococcus xanthus*. *J. Bacteriol.* **181**: 4381-4390.

93. **Rodriguez-Soto, J.P., and Kaiser, D.** (1997) Identification and localization of the Tgl protein, which is required for *Myxococcus xanthus* social motility. *J Bacteriol* **179**: 4372-4381.

94. **Rosenberg, E., Fytlovitch, S., Carmeli, S., and Kashman, Y.** (1982) Chemical properties of *Myxococcus xanthus* antibiotic TA. *J. Antibiot.* **35**: 788-793.

95. **Rosenbluh, A., Nir, R., Sahar, E., and Rosenberg, E.** (1989) Cell-density-dependent lysis and sporulation of *Myxococcus xanthus* in agarose microbeads. *J. Bacteriol.* **171**: 4923-4929.

96. **Russo-Marie, F., Roederer, M., Sager, B., Herzenberg, L.A., and Kaiser, D.** (1993) β-galactosidase activity in single differentiating bacterial cells. *Proc. Natl. Acad. Sci. USA* **90**: 8194-8198.

97. **Shi, W., Kohler, T., and Zusman, D.R.** (1993) Chemotaxis plays a role in the social behavior of *Myxococcus xanthus*. *Molec. Microbiol.* **9**: 601-611.

98. **Shimkets, L.J.** Unpublished data.

99. **Shimkets, L.J., Gill, R.E., and Kaiser, D.** (1983) Developmental cell interactions in *Myxococcus xanthus* and the *spoC* locus. *Proc. Natl. Acad. Sci. USA* **80**: 1406-1410.

100. **Shimkets, L.J., and Asher, S.J.** (1988) Use of recombination techniques to examine the structure of the *csg* locus of *Myxococcus xanthus*. *Mol. Gen. Genet.* **211**: 63-71.

101. **Shimkets, L.J.** (1990) Social and developmental biology of the myxobacteria. *Microbiol. Rev.* **54**: 473-501.

102. **Shimkets, L.J., and Rafiee, H.** (1990) CsgA, an extracellular protein essential for *Myxococcus xanthus* development. *J. Bacteriol.* **172**: 5299-5306.

103. **Shimkets, L.J.** (1999) Intercellular signaling during fruiting body development of *Myxococcus xanthus*. *Annu. Rev. Microbiol.* **53**: 525-549.

104. **Shimkets, L.J., and Kaiser, D.** (1999) Cell contact-dependent C signaling in *Myxococcus xanthus*. In *Cell-cell signaling in bacteria*. Dunny, G.M. and Winans, S.C. (eds). Washington, D. C.: American Society for Microbiology, pp. 83-97.

105. **Simunovic, V.** Unpublished results.

106. **Skerker, J.M., and Berg, H.C.** (2001) Direct observation of extension and retraction of type IV pili. *Proc. Natl. Acad. Sci. USA* **98**: 6901-6904.

107. **Sogaard-Andersen, L., and Kaiser, D.** (1996) C-factor, a cell-surface-associated intercellular signaling protein, stimulates the cytoplasmic Frz signal transduction system in *Myxococcus xanthus*. *Proc. Natl. Acad. Sci. USA* **93**: 2625-2679.

108. **Stauton, J., and Wilkinson, B.** (1997) Biosynthesis of erythromycin and rapamycin. *Chem. Rev.* **97**: 2611-2629.

109. **Sudo, S.Z., and Dworkin, M.** (1969) Resistance of vegetative cells and microcysts of *Myxococcus xanthus*. *J. Bacteriol.* **98**: 883-887.

110. **Sun, H., Zusman, D.R., and Shi, W.** (2000) Type IV pilus of *Myxococcus xanthus* is a motility apparatus controlled by the *frz* chemosensory system. *Current Biology* **10**: 1143-1146.

111. **Thony-Meyer, L., and Kaiser, D.** (1993) *devRS*, an autoregulated and essential genetic locus for fruiting body development in *Myxococcus xanthus*. *J. Bacteriol.* **175**: 7450-7462.

112. **Toal, D.R., Clifton, S.W., Roe, B.R., and Downard, J.** (1995) The *esg* locus of *Myxococcus xanthus* encodes the E1α and E1ß subunits of a branched-chain keto acid dehydrogenase. *Molec. Microbiol.* **16**: 177-189.

113. **Tojo, N., Inouye, S., and Komano, T.** (1993) The *lonD* gene is homologous to the *lon* gene encoding an ATP-dependent protease and is essential for the development of *Myxococcus xanthus*. *J. Bacteriol.* **175**: 4545-4549.

114. **Towbin, H., Staehelin, T., and Gordon, J.** (1979) Electrophoretic transfer of proteins from polyacrylamide gels to nitrocellulose sheets: procedure and some applications. *Proc. Natl. Acad. Sci USA* **76**: 4350-4354.

115. **Trowitzsch, W., Wray, V., Gerth, K., and Hofle, G.** (1982) Structure of myxovirescen A, a new macrocyclic antibiotic from gliding bacteria. *J.Chem. Soc. Chem Commun.* **1982**: 1340-1342.

116. **Van Delden, C., Comte, R., and Bally, M.** (2001) Stringent response activates quorum sensing and modulates cell density-dependent gene expression in *Pseudomonas aeruginosa*. *J. Bacteriol.* **183**: 5376-5384.

117. **Voelz, H., and Dworkin, M.** (1962) The fine structure of a fruiting myxobacterium. *Fifth Internatl. Congress for Electron Microscopy*.

118. **Walker, J.E., Saraste, M., Runswick, M.J., and Gay, N.J.** (1982) Distantly related sequences in the alpha- and beta-subunits of ATP synthase, myosin and

other ATP-requiring enzymes and a common nucleotide binding fold. *EMBO J* **1**: 945-951.

119. **Wall, D., Wu, S.S., and Kaiser, D.** (1998) Contact stimulation of Tgl and type IV pili in *Myxococcus xanthus*. *J. Bacteriol.* **180**: 759-761.

120. **Ward, M.J., and Zusman, D.R.** (1999) Motility in *Myxococcus xanthus* and its role in developmental aggregation. *Cur. Opin. Microbiol.* **2**: 624-629.

121. **Wedel, A., Weiss, D.S., Popham, D., Droge, P., and Kustu, S.** (1990) A bacterial enhancer functions to tether a transcriptional activator near a promoter. *Science* **248**: 486-490.

122. **Weimer, R.M., C. Creighton, A. Stassinopoulos, P. Youderian, and Hartzell, P.** (1998) A chaperone in the HSP70 family controls production of extracellular fibrils in *Myxococcus xanthus*. *J. Bacteriol.* **180**: 5357-5368.

123. **White, D., Dworkin, M., and Tipper, D.J.** (1968) Peptidoglycan of *Myxococcus xanthus*: Structure and relation to morphogenesis. *J. Bacteriol.* **95**: 2186-2197.

124. **White, D.J., and Hartzell, P.L.** (2000) AglU, a protein required for gliding motility and spore maturation of *Myxococcus xanthus*, is related to WD-repeat proteins. *Mol. Microbiol.* **36**: 662-678.

125. **Wolgemuth, C., Hoiczyk, E., Kaiser, D., and Oster, G.** (2002) How myxobacteria glide. *Curr. Biol.* **12**: 369-377.

126. **Wu, S.S., and Kaiser, D.** (1995) Genetic and functional evidence that Type IV pili are required for social gliding motility in *Myxococcus xanthus* **18**: 547-558.

127. **Wu, S.S., and Kaiser, D.** (1997) Regulation of expression of the *pilA* gene of *Myxococcus xanthus*. *J. Bacteriol.* **179**: 7748-7758.

128. **Wu, S.S., Wu, J., Cheng, Y., and Kaiser, D.** (1998) The *pilH* gene encodes an ABC transporter homologue required for type IV pilus biogenesis and social gliding motility in *Myxococcus xanthus*. *Molec. Microbiol.* **29**: 1249-1261.

129. **Yang, C., and Kaplan, H.B.** Unpublished data.

130. **Zafriri, D., Rosenberg, E., and Mirelman, D.** (1981) Mode of action of *Myxococcus xanthus* antibiotic TA. *Antimicrobial Agents and Chemotherapy* **19**: 349-351.

131. **Zocher, R., and Keller, U.** (1997) Thiol template peptide synthesis systems in bacteria and fungi. *Adv. in Microb. Physiol.* **38**: 85-131.

132. **Zusman, D.R.** (1982) Frizzy mutants: a new class of aggregation-defective developmental mutants of *Myxococcus xanthus*. *J. Bacteriol.* **150**: 1430-1437.

133. **Zusman, D.R.** (1984) Developmental program of *Myxococcus xanthus*. In *Myxobacteria Development and Cell Interactions*, pp. 185-213.

Table 1.1 Genes of *M. xanthus* representing different extracellular complementation groups

Complementation group	Gene symbol	Gene product function	Complementing fraction
A	*asgA*	Histidine protein kinase/ response regulator	Amino acid mixture
	asgB	Putative transcription factor	
	asgC	Sigma-70 transcription factor	
	asgD	Receiver domain/histidine protein kinase	
	asgE	unknown	
B	*bsg*	Lon-type protease	unknown
C	*csgA*	Short chain alcohol dehydrogenase	CsgA
D	*dsg*	Translation initiation factor (IF 3)	Mixture of fatty acids and autolysins
E	*esg*	E1α and E1β subunits of branched-chain keto acid dehydrogenase	Isovalerate
S	*sgl, dsp, rfb ABC*	Social motility	Fibrils

Table 3.1 Physical, biochemical and immunological properties of *M. xanthus* DK1622 membrane peaks

			(% recovered ± SD)[a]		
Peak	[b]Peak density (g/ml)	SDH	Lipid A	Protein	Designation
I	1.292-1.310	25 ± 1.0	16 ± 5.7	42 ± 3.6	IM
II	1.252-1.258	11 ± 2.0	8.0 ± 5.6	16 ± 4.4	HM
IV	1.197	62 ± 1.6	48 ± 8.0	32 ± 1.2	HM
V	1.213-1.240	1.3 ± 0.6	14 ± 7.8	4.3 ± 1.5	OM
VI	1.169-1.171	1.0 ± 0.0	14 ± 5.7	6.3 ± 2.5	OM

[a] Percentage of the total amount of marker (protein) recovered in membrane peak/ total amount of marker (protein) recovered from all the peaks on the gradient. Values represent the averages of three independent experiments ± standard deviations (SD).

[b] Values represent the range of peak densities determined by A_{280} from three gradients.

Figure 1.1 The C-signal transduction pathway. Low to intermediate levels of C-signal activate the FruA response regulator, that consequently activates the Frz signal transduction system to modulate cell motility. High levels of C-signal are channeled through *devRS* and other late developmental genes to induce sporulation. The *act* operon controls the timing and expression of *csgA*. The big arrows indicate C-signal input and output.

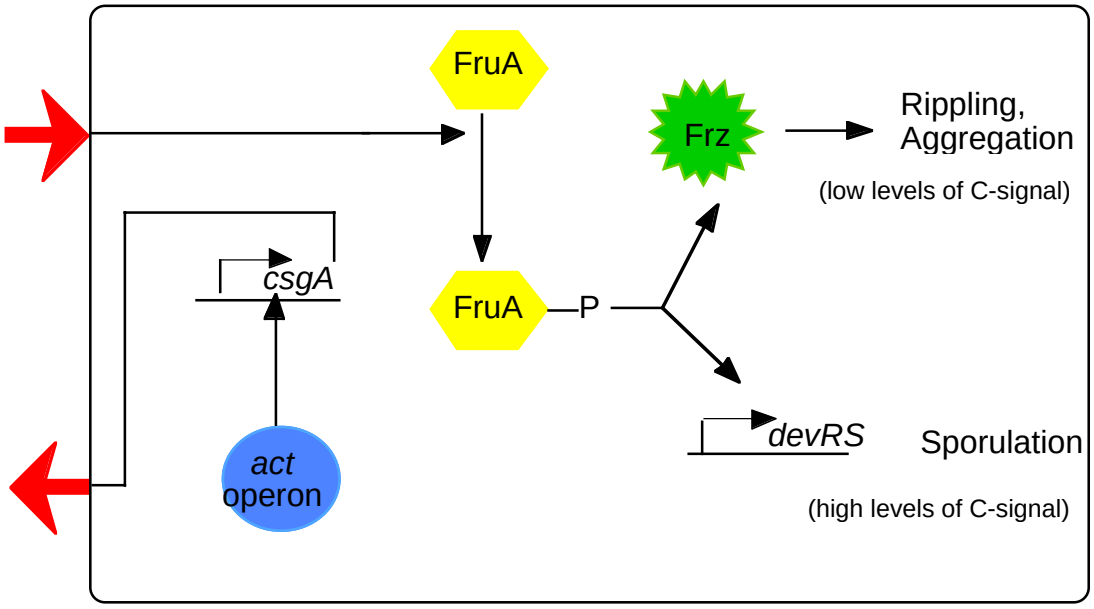
FruA
Frz
Rippling,
Aggregation
(low levels of C-signal)
csgA
FruA
P
devRS
Sporulation
act
operon
(high levels of C-signal)

Figure 3.1 Scheme for separating membranes of *M. xanthus* DK1622 vegetative cells. Membranes were prepared as outlined in Materials and Methods. Total membranes were separated on a three-step sucrose gradient (3 h at 100,000 x g) (A). Each membrane enrichment (heavy, medium, and light) was concentrated (B). Heavy and medium membrane enrichments were concentrated for 3 h, while the light membrane enrichment was concentrated for 6 h (100,000 x g). Concentrated membrane fractions were diluted in a small volume of buffer and separated on discontinuous sucrose gradients (C). The peaks are indicated by Roman numerals I through VII.

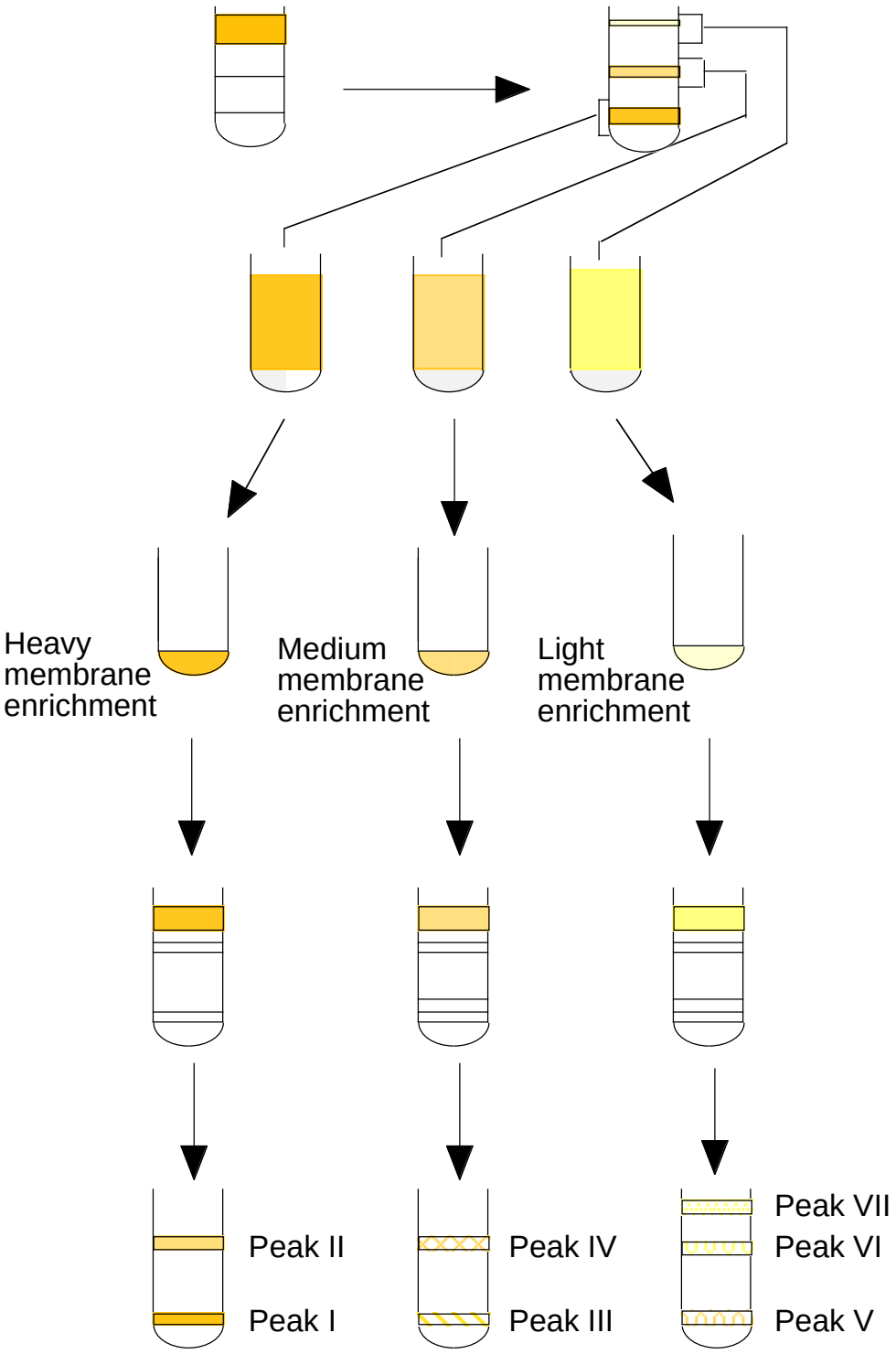
Heavy membrane enrichment
Medium membrane enrichment
Light membrane enrichment
Peak II
Peak I
Peak IV
Peak III
Peak VII
Peak VI
Peak V

Figure 3.2 Graphical representation of heavy membrane (A), medium membrane (B), and the light membrane peaks (C) on discontinuous sucrose gradients as a function of relative protein content (A_{280}), (squares), and buoyant density, (diamonds). Fractions under each peak were consolidated, harvested by ultracentrifugation, and submitted to biochemical and immunoblot analysis.

A)

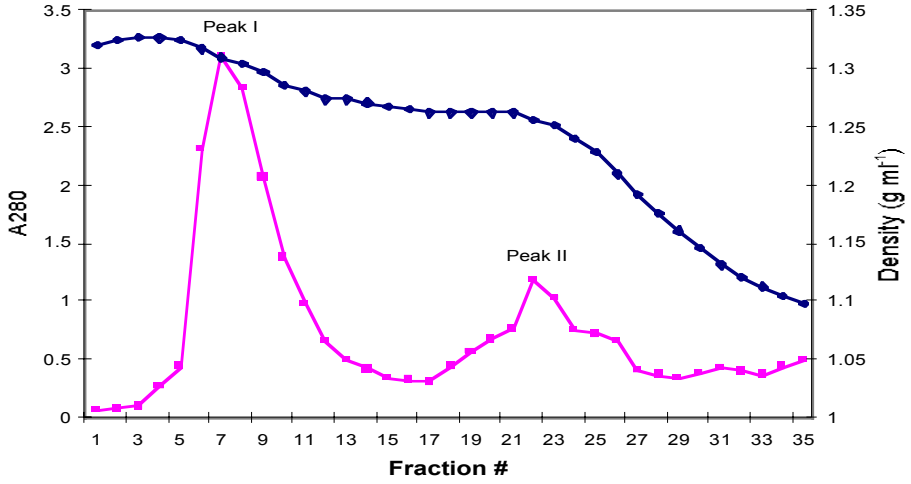
Peak I
Peak II
A280
Density (g ml-1)
Fraction #

B)

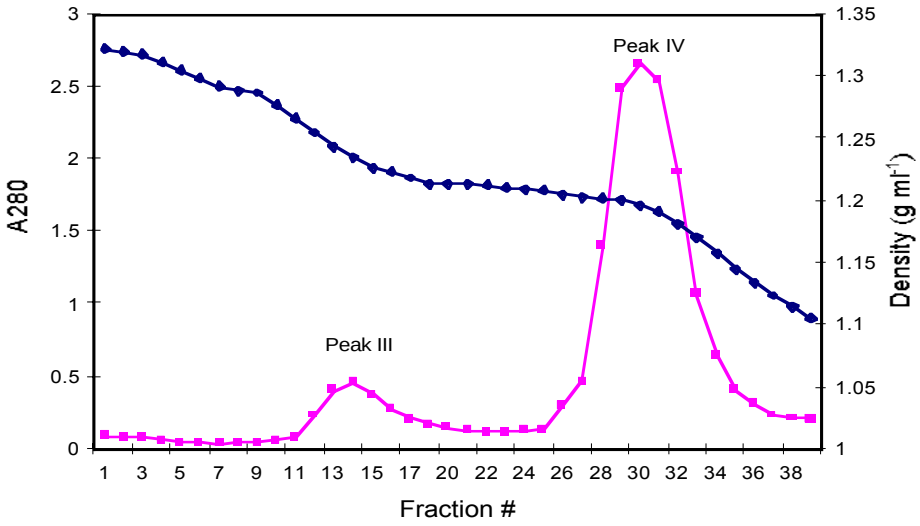
Peak III
Peak IV
A280
Density (g ml-1)
Fraction #

C)

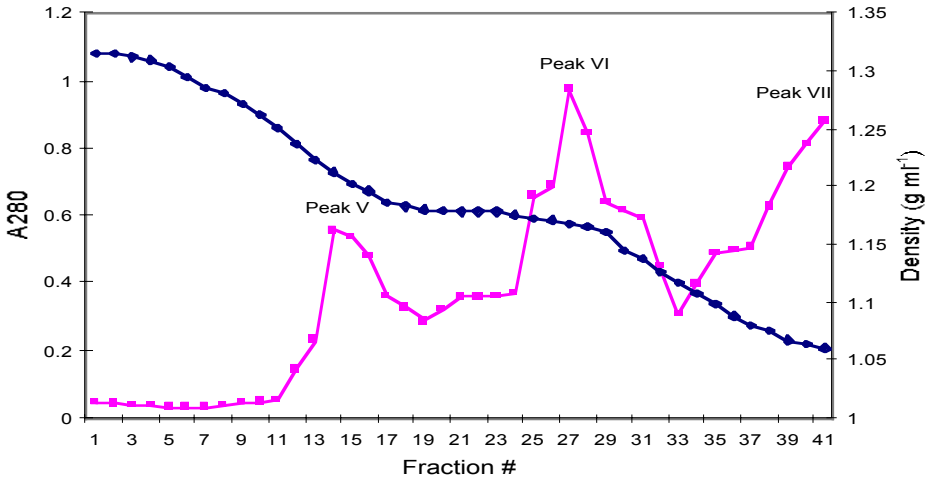
Peak V
Peak VI
Peak VII
A280
Density (g ml-1)
Fraction #

Figure 3.3 Immunoblots of isolated membrane fractions displaying lipid A, (A); LPS O-antigen, (B); Tgl, a lipoprotein required for assembly of type IV pili, (C); PilA, the structural pilin protein, (D); FibA, an extracellular matrix-associated zinc metalloprotease, (E); CsgA, a protein required for C-signal production, (F); and FrzCD, a methylated chemotaxis protein, (G). Total membrane (TM), inner membrane, peak I (I), hybrid membrane 1, peak II (II), hybrid membrane 2, peak IV (IV), outer membrane 1, peak V(V), and outer membrane 2, peak VI (VI) fractions were separated by SDS-PAGE for Western blotting. Numbers on the left indicate the molecular weight of each antigen in kDa.

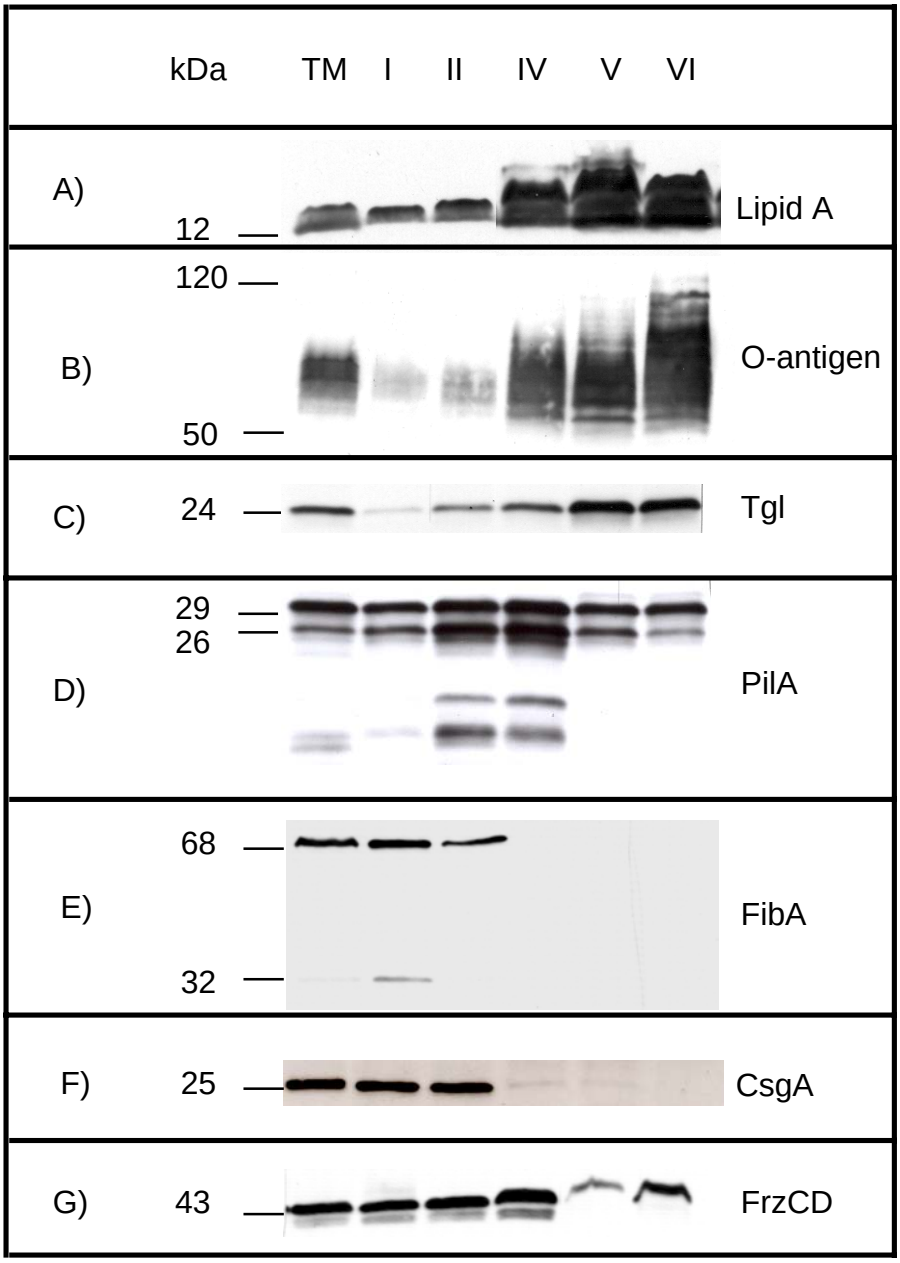
kDa
TM
I
II
IV
V
VI
A)
12
Lipid A
120
50
B)
O-antigen
C)
24
Tgl
29
26
D)
PilA
68
E)
32
FibA
F)
25
CsgA
G)
43
FrzCD

Figure 3.4 Two dimensional SDS-PAGE separated in the first dimension at pH 3.5-10 and in the second dimension on 10% polyacrylamide. Inner membrane, peak I (A), hybrid membrane 2, peak IV (B), outer membrane 1, peak V (C), and outer membrane 2, peak VI (D). Molecular weight markers are indicated on the left. A series of internal, carbamylated carbonic anhydrase markers ranging from 5.0 to 7.3 pH are underlined on each gel. Rectangles indicate acidic proteins common to the inner membrane which do not resolve properly. Arrows pointing down in Panel A indicate protein spots common to peaks I and VI. Arrows pointing up in Panel B indicate proteins common to peaks V and VI. Numbers 1-5 indicate clusters of proteins differentially expressed in the two outer membrane peaks.

A)

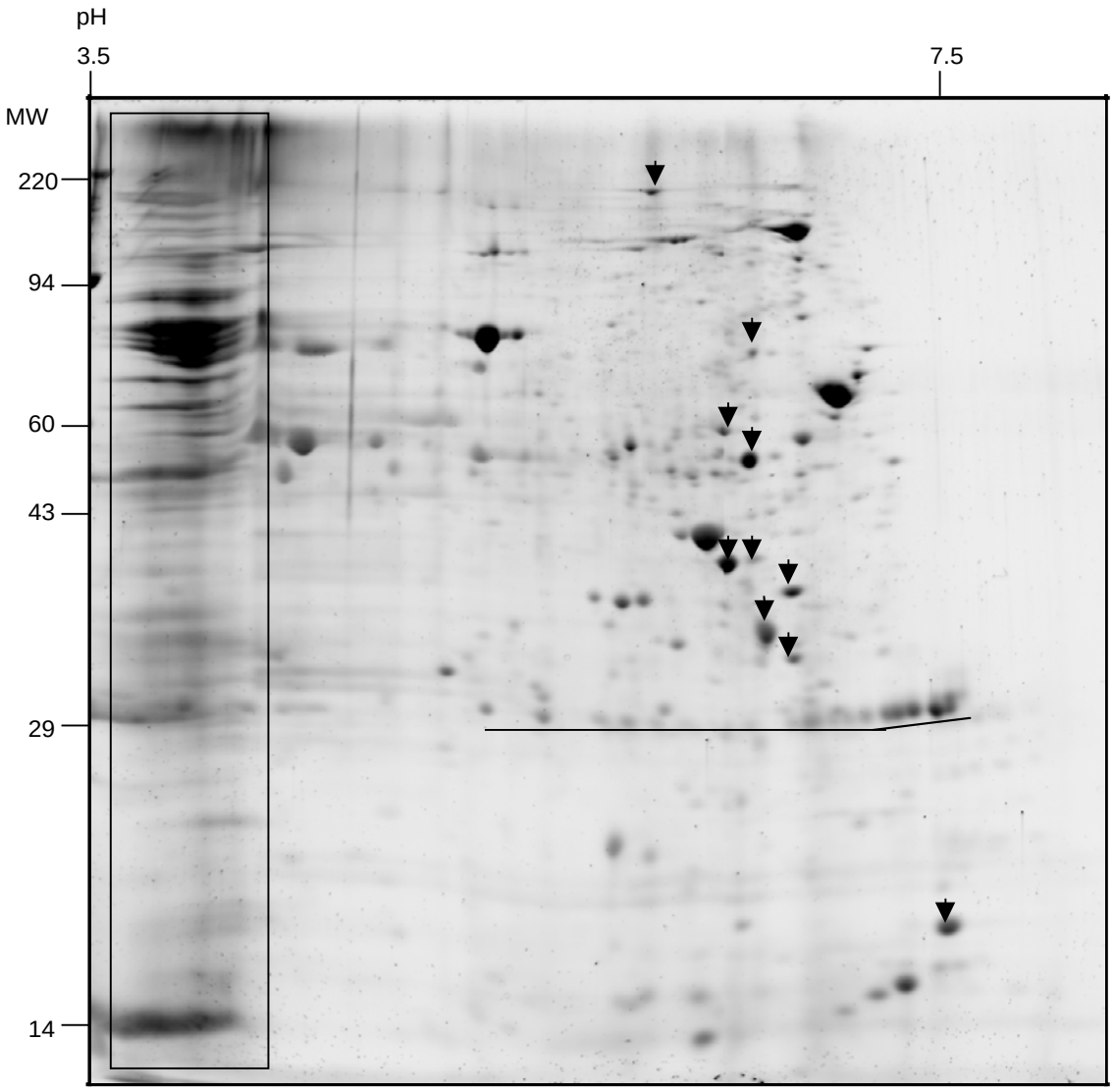

B)

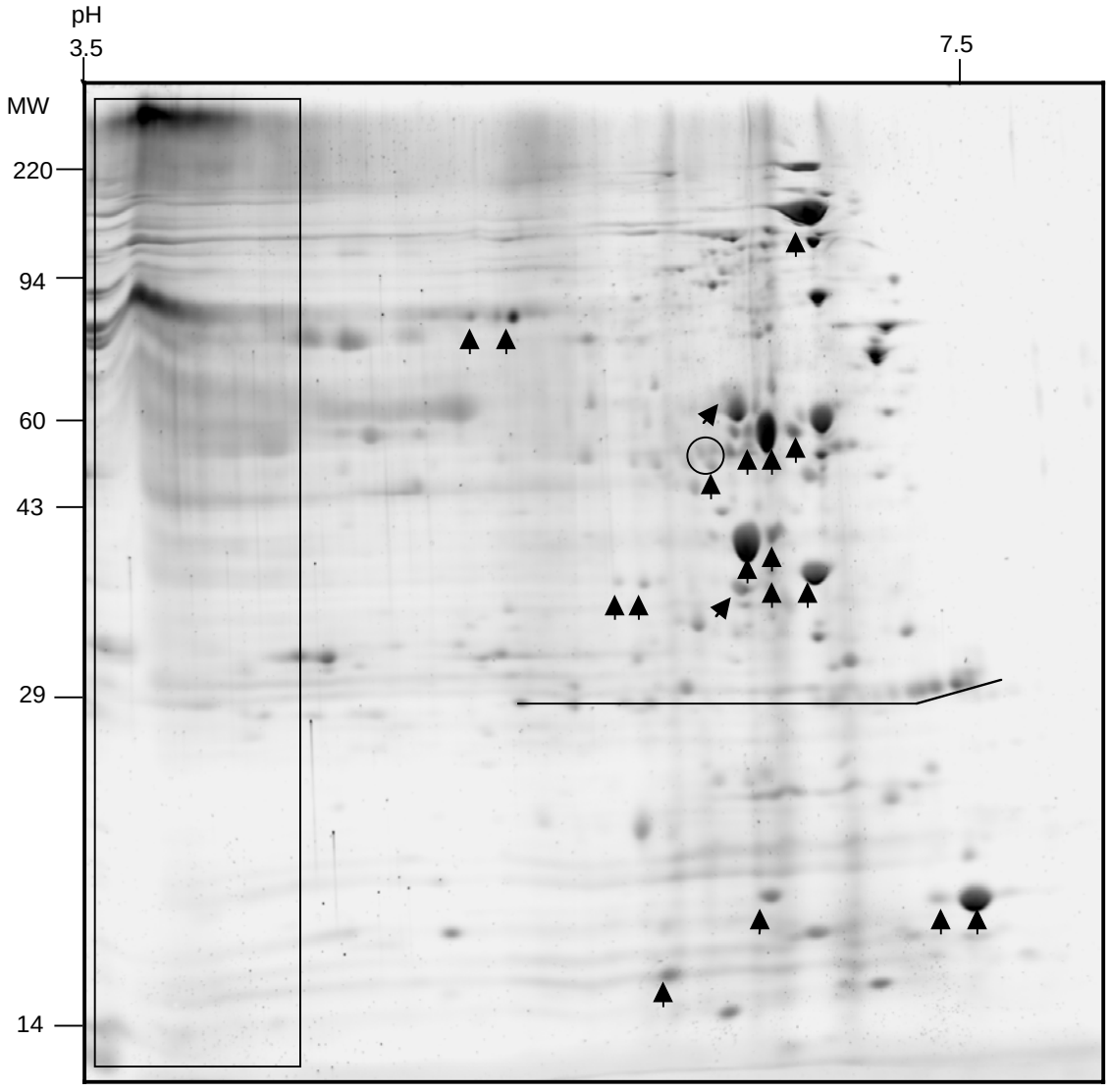

C)

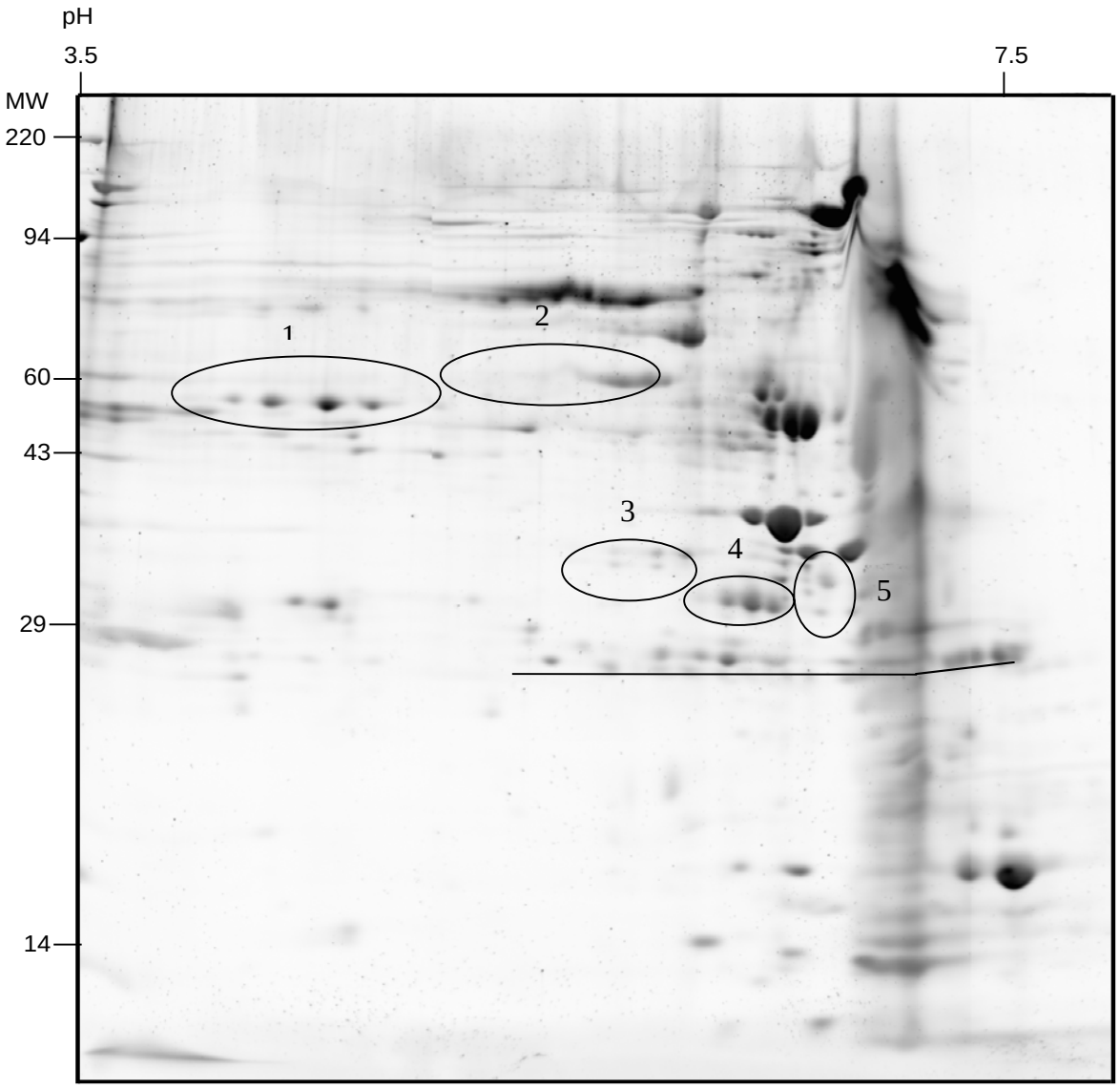

D)

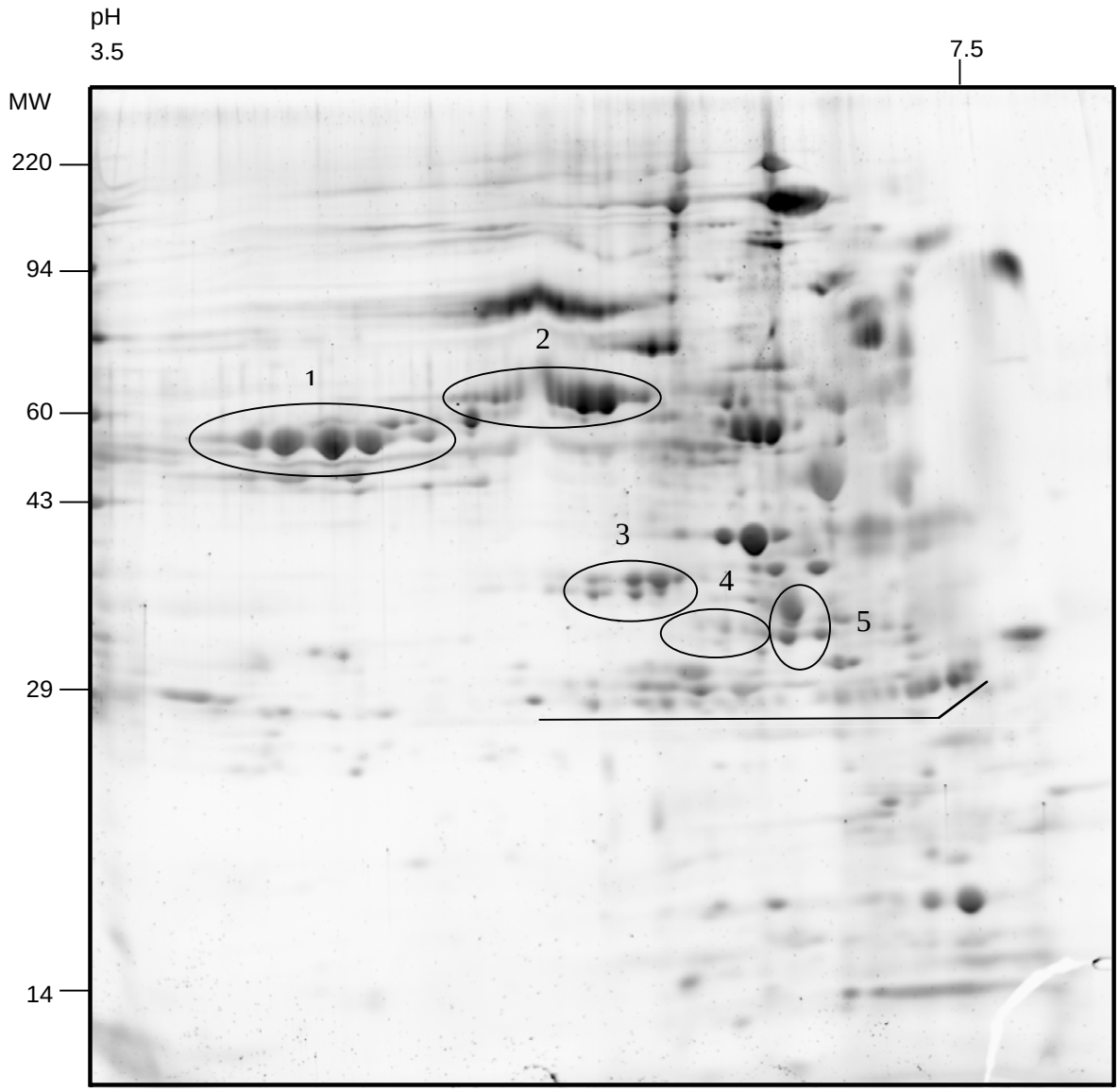

Figure 3.5 A) 7.5 % polyacrylamide gel of fraction VII stained with Coomassie blue. Stars indicate protein bands analyzed by MALDI-TOF MS. B) Predicted organization of the 7831 amino acid Ta-1 polyketide synthetase (PKS). Conserved domains are as follows: condensation domain (C), activation domain (A), β-keto synthase/ acyl transferase (KS/AT), β-keto reductase (KR), and acyl carrier protein (ACP) domains. Domains are organized in modules, basic units responsible for incorporation of extender units. The scale bar indicates the amino acid number within the primary structure of Ta-1.

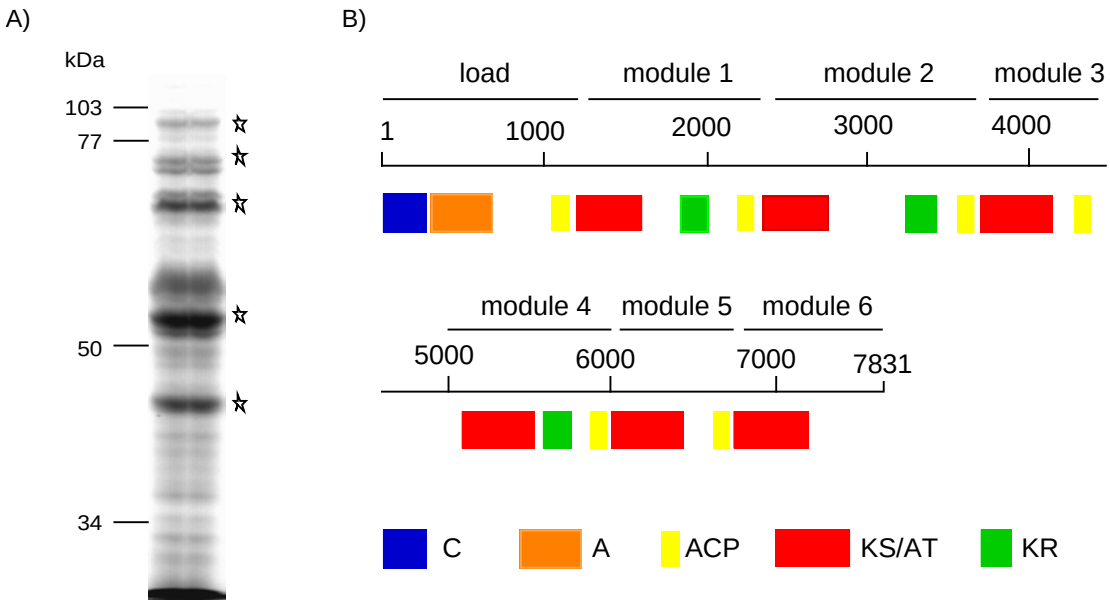
A)
kDa
103
77
50
34
B)
load
module 1
module 2
module 3
1
1000
2000
3000
4000
module 4
module 5
module 6
5000
6000
7000
7831
C
A
ACP
KS/AT
KR